

LUNG DISEASE

A PI3K γ mimetic peptide triggers CFTR gating, bronchodilation, and reduced inflammation in obstructive airway diseases

Alessandra Ghigo^{1,2,*†}, Alessandra Murabito^{1†}, Valentina Sala^{1,2}, Anna Rita Pisano³, Serena Bertolini³, Ambra Gianotti⁴, Emanuela Caci⁴, Alessio Montresor^{5,6}, Aiswarya Premchandrar⁷, Flora Pirozzi^{1,8}, Kai Ren¹, Angela Della Sala¹, Marco Mergioti¹, Wito Richter⁹, Eyleen de Poel¹⁰, Michaela Matthey¹¹, Sara Calderer^{5,6‡}, Rosa A. Cardone¹², Federica Civiletti¹³, Andrea Costamagna¹³, Nancy L. Quinney¹⁴, Cosmin Butnaru¹, Sonja Visentin¹, Maria Rosaria Ruggiero¹, Simona Baroni¹, Simonetta Geninatti Crich¹, Damien Ramel¹⁵, Muriel Laffargue¹⁵, Carlo G. Tocchetti^{8,16,17}, Renzo Levi¹⁸, Marco Conti¹⁹, Xiao-Yun Lu²⁰, Paola Melotti²¹, Claudio Sorio^{5,6}, Virginia De Rose¹, Fabrizio Facchinetti³, Vito Fanelli¹³, Daniela Wenzel^{11,22}, Bernd K. Fleischmann²², Marcus A. Mall^{23,24}, Jeffrey Beekman¹⁰, Carlo Laudanna^{5,6}, Martina Gentzsch^{14,25}, Gergely L. Lukacs⁷, Nicoletta Pedemonte⁴, Emilio Hirsch^{1,2,*}

Copyright © 2022
The Authors, some
rights reserved;
exclusive licensee
American Association
for the Advancement
of Science. No claim
to original U.S.
Government Works

Cyclic adenosine 3',5'-monophosphate (cAMP)-elevating agents, such as β_2 -adrenergic receptor (β_2 -AR) agonists and phosphodiesterase (PDE) inhibitors, remain a mainstay in the treatment of obstructive respiratory diseases, conditions characterized by airway constriction, inflammation, and mucus hypersecretion. However, their clinical use is limited by unwanted side effects because of unrestricted cAMP elevation in the airways and in distant organs. Here, we identified the A-kinase anchoring protein phosphoinositide 3-kinase γ (PI3K γ) as a critical regulator of a discrete cAMP signaling microdomain activated by β_2 -ARs in airway structural and inflammatory cells. Displacement of the PI3K γ -anchored pool of protein kinase A (PKA) by an inhaled, cell-permeable, PI3K γ mimetic peptide (PI3K γ MP) inhibited a pool of subcortical PDE4B and PDE4D and safely increased cAMP in the lungs, leading to airway smooth muscle relaxation and reduced neutrophil infiltration in a murine model of asthma. In human bronchial epithelial cells, PI3K γ MP induced unexpected cAMP and PKA elevations restricted to the vicinity of the cystic fibrosis transmembrane conductance regulator (CFTR), the ion channel controlling mucus hydration that is mutated in cystic fibrosis (CF). PI3K γ MP promoted the phosphorylation of wild-type CFTR on serine-737, triggering channel gating, and rescued the function of F508del-CFTR, the most prevalent CF mutant, by enhancing the effects of existing CFTR modulators. These results unveil PI3K γ as the regulator of a β_2 -AR/cAMP microdomain central to smooth muscle contraction, immune cell activation, and epithelial fluid secretion in the airways, suggesting the use of a PI3K γ MP for compartment-restricted, therapeutic cAMP elevation in chronic obstructive respiratory diseases.

INTRODUCTION

Obstructive airway diseases, including asthma, chronic obstructive pulmonary disease (COPD) and the genetic disorder cystic fibrosis (CF), represent a major health burden worldwide. Over the next decade, prevalence of asthma and COPD is predicted to rise in developing countries (1) and so is the number of patients with CF requiring

long-term care, because survival is progressively improving due to better treatments and intensive follow-up (2). Despite the diversity in etiology, pathogenetic mechanisms, and clinical manifestations, these conditions share common features such as chronic airway inflammation, mucus hypersecretion, and airflow obstruction due to airway hyperreactivity and/or mucus plugging (1, 2). Conventional

¹Department of Molecular Biotechnology and Health Sciences, Molecular Biotechnology Center, University of Torino, 10126 Torino, Italy. ²Kither Biotech Srl, 10126, Torino, Italy. ³Chiesi Farmaceutici S.p.A., Corporate Pre-Clinical R&D, 43122 Parma, Italy. ⁴UOC Genetica Medica, IRCCS Istituto Giannina Gaslini, 16147 Genova, Italy. ⁵Division of General Pathology, Department of Medicine, University of Verona School of Medicine, 37134 Verona, Italy. ⁶Cystic Fibrosis Translational Research Laboratory "Daniele Lissandrini," Department of Medicine, University of Verona School of Medicine, 37134 Verona, Italy. ⁷Department of Physiology, McGill University, Montréal, Québec H3G 1Y6, Canada. ⁸Department of Translational Medical Sciences, Federico II University, 80131 Naples, Italy. ⁹Department of Biochemistry and Molecular Biology, University of South Alabama College of Medicine Mobile, AL 36688, USA. ¹⁰Department of Pediatric Pulmonology, Wilhelmina Children's Hospital, University Medical Center Utrecht, 3584 EA Utrecht, Netherlands. ¹¹Department of Systems Physiology, Medical Faculty, Ruhr University Bochum, 44801 Bochum, Germany. ¹²Department of Biosciences, Biotechnologies, and Biopharmaceutics, University of Bari, 70126 Bari, Italy. ¹³Department of Anesthesia and Critical Care Medicine, University of Torino, Azienda Ospedaliera Città della Salute e della Scienza di Torino, 10126 Torino, Italy. ¹⁴Marsico Lung Institute/Cystic Fibrosis Research Center, University of North Carolina, Chapel Hill, NC 27599, USA. ¹⁵Institute of Metabolic and Cardiovascular Diseases, Paul Sabatier University, 31432 Toulouse, France. ¹⁶Interdepartmental Center of Clinical and Translational Research (CIRCET), Federico II University, 80131 Naples, Italy. ¹⁷Interdepartmental Hypertension Research Center (CIRIAPA), Federico II University, 80131 Naples, Italy. ¹⁸Department of Life Sciences and Systems Biology, University of Torino, 10123 Torino, Italy. ¹⁹Department of Obstetrics, Gynecology, and Reproductive Sciences, University of California San Francisco, San Francisco, CA 94143, USA. ²⁰School of Life Science and Technology, Xi'an Jiaotong University, 710049 Xi'an Shaanxi, P.R. China. ²¹Cystic Fibrosis Center, Azienda Ospedaliera Universitaria Integrata di Verona, 37126 Verona, Italy. ²²Institute of Physiology I, Life and Brain Center, Medical Faculty, University of Bonn, 53127 Bonn, Germany. ²³Department of Pediatric Respiratory Medicine, Immunology, and Critical Care Medicine, Charité-Universitätsmedizin Berlin, 10117 Berlin, Germany. ²⁴German Center for Lung Research (DZL), associated partner, 10117 Berlin, Germany. ²⁵Department of Pediatric Pulmonology, University of North Carolina, Chapel Hill, NC 27599, USA. *Corresponding author. Email: alessandra.ghigo@unito.it (A.G.); emilio.hirsch@unito.it (E.H.)

†These authors contributed equally to this work.

‡Present address: Department of Infectious, Tropical Diseases and Microbiology, IRCCS Sacro Cuore Don Calabria Hospital, 37024 Negrar, Italy.

medications, especially for asthma, include inhaled corticosteroids and β_2 -adrenergic receptor (β_2 -AR) agonists, which reduce airway inflammation and reverse airway constriction, respectively (1). Whereas the primary effect of β_2 -AR agonists is relaxation of airway smooth muscle, these drugs can also engage this receptor in infiltrating leukocytes, eventually contributing to the resolution of inflammation through the cyclic adenosine 3',5'-monophosphate (cAMP) pathway (3). Furthermore, β_2 -AR agonists are potent inducers of the CF transmembrane conductance regulator (CFTR) (4), the epithelial anion channel that drives airway surface fluid hydration. CFTR dysfunction is a major cause of mucus hyperconcentration that leads to impaired mucociliary clearance and mucus plugging not only in patients with the genetic disorder CF (2) but also in COPD (5) and asthma (6). Although β_2 -AR agonists could be beneficial in these chronic obstructive diseases, their efficacy is still limited, primarily because of tachyphylaxis and adverse events, such as tachyarrhythmias, stemming from systemic drug exposure. Similarly, inhibition of cAMP breakdown by drugs targeting phosphodiesterase 4 (PDE4) (7), the major cAMP-hydrolyzing enzyme in the airways, is clinically effective but exhibits unwanted side effects, such as emesis, diarrhea, and weight loss, likely due to systemic PDE4 blockade (8). Thus, safer approaches for the manipulation of the β_2 -AR/cAMP signaling axis for the treatment of chronic airway diseases are desirable.

Previous work from our group identified phosphoinositide 3-kinase γ (PI3K γ) as a negative regulator of β_2 -AR/cAMP signaling in the heart. In this tissue, PI3K γ serves as an A-kinase anchoring protein (AKAP) that tethers protein kinase A (PKA) to PDE3 and PDE4, favoring their PKA-mediated phosphorylation and activation. This mechanism of localized PDE stimulation eventually allows restricting β_2 -AR/cAMP responses to discrete subcellular compartments (9, 10). Accordingly, disruption of the scaffold but not the kinase activity of PI3K γ results in β_2 -AR/cAMP signaling amplification in cardiomyocytes (9). Because PI3K γ is also found in pulmonary cells (11), we speculated that PI3K γ could contribute to the compartmentalization of β_2 -AR/cAMP responses in the lungs and that pharmacological targeting of PI3K γ scaffold activity could achieve therapeutic cAMP elevation in the airways.

Here, we described a cell-permeable PI3K γ -derived mimetic peptide (PI3K γ MP) that, by interrupting the interaction between PI3K γ and PKA, inhibited PI3K γ -associated PDE4B and PDE4D and, in turn, enhanced β_2 -AR/cAMP responses in human bronchial smooth muscle, epithelial, and immune cells. Intratracheal instillation of PI3K γ MP limited bronchoconstriction and lung neutrophil infiltration in a mouse model of asthma. In human airway epithelial cells, PI3K γ MP promoted gating of wild-type (wt) CFTR and restored the function of the most prevalent CFTR mutant in CF (F508del) by potentiating the effects of approved CFTR modulators.

RESULTS

A PI3K γ MP enhances airway β_2 -AR/cAMP signaling

To assess the role of PI3K γ scaffold activity in the regulation of airway cAMP, we compared PI3K γ knockout mice (PI3K $\gamma^{-/-}$), lacking both the anchoring and the catalytic function of the p110 γ subunit of PI3K γ , with animals expressing a kinase-inactive p110 γ that retains the scaffold activity [PI3K γ kinase-dead (PI3K $\gamma^{KD/KD}$)] (9). The amount of cAMP was twofold higher in PI3K $\gamma^{-/-}$ than in wt (PI3K $\gamma^{+/+}$) and PI3K $\gamma^{KD/KD}$ tracheas (Fig. 1A), suggesting a kinase-

independent control of airway cAMP by PI3K γ . Similar to previous findings in the heart (9), the increased cAMP concentration detected in PI3K $\gamma^{-/-}$ tracheas correlated with reduced activity of PDE4B and PDE4D, whereas their function was normal in PI3K $\gamma^{KD/KD}$ tissues (Fig. 1B). Modulation of PDE4B and PDE4D by PI3K γ was also detected in isolated murine tracheal smooth muscle cells (mTSMCs) (Fig. 1C), where PI3K γ was found to be highly abundant (Fig. 1D). As shown in Fig. 1D, the canonical p110 γ doublet was detectable in peripheral blood mononuclear cells and tracheas, whereas mTSMCs and human bronchial smooth muscle cells (hBSMCs) displayed the low-molecular weight isoform only. These PI3K γ forms were found to organize multiprotein complexes containing both PDEs and their activator PKA (Fig. 1, E and F). Down-regulation of the *PIK3CG* gene (encoding p110 γ) in hBSMCs increased β_2 -AR-activated cAMP responses by 30% (Fig. 1G), thus supporting a PI3K γ kinase-independent activation of PDE4, restraining airway cAMP downstream of β_2 -ARs.

These findings prompted us to design a molecule interfering with the scaffold function of PI3K γ and enhancing β_2 -AR/cAMP signaling in the airways. To disrupt the PKA-anchoring function of PI3K γ in vivo, a peptide encompassing the PKA-binding motif of PI3K γ (10) was fused to the cell-penetrating sequence penetratin-1 (P1) (Fig. 2A) (12). A fluorescein isothiocyanate (FITC)-labeled version of this PI3K γ MP was detectable in hBSMCs within 30 min of administration (Fig. 2A). PI3K γ MP associated the recombinant RII α subunit of PKA with a dissociation constant of 7.5 μ M (Fig. 2B) and dose-dependently disrupted the PKA-RII/p110 γ interaction (Fig. 2C). Conversely, PI3K γ MP did not alter C5a-mediated Akt phosphorylation (fig. S1A), indicating that it did not interfere with the kinase function of PI3K γ (9). In line with the ability to disturb PKA/p110 γ association, PI3K γ MP reduced PDE4B and PDE4D activity by 30% in primary wt mTSMCs, whereas no significant effect of the peptide was observed in PI3K γ -deficient cells ($P > 0.9999$) (Fig. 2D). Similarly, PI3K γ MP failed to increase cAMP in PI3K $\gamma^{-/-}$ macrophages (fig. S1B), confirming that PI3K γ MP specifically inhibited PI3K γ -associated PDEs but not PDEs anchored to other AKAPs (7). In hBSMCs, PI3K γ MP, but not a control peptide (CP) containing P1 only, increased β_2 -AR-evoked cAMP responses by 35% (Fig. 2E). Furthermore, PI3K γ MP induced cAMP elevation in human airway epithelial cells (16HBE14o-) with a maximal effective concentration of 21.66 μ M (Fig. 2F), whereas a CP containing P1 fused to a scrambled sequence of the PKA-binding site of p110 γ failed to affect cAMP abundance (fig. S1C).

To assess whether PI3K γ MP could enhance airway β_2 -AR/cAMP signaling in vivo, the peptide was instilled intratracheally in mice and found to induce a dose-dependent increase in cAMP, with 80 μ g/kg as the lowest dose eliciting a significant increase in cAMP concentration in both tracheas ($P < 0.0001$) and lungs ($P = 0.0288$) (Fig. 3A). Mice receiving FITC-labeled PI3K γ MP (80 μ g/kg) showed fluorescence in the airways as soon as 30 min after a single intratracheal administration (fig. S2A) when the amount of cAMP was already 30% higher than in tissues from animals receiving either saline or CP (fig. S2B). Moreover, PI3K γ MP persisted in the airways up to 24 hours after a single-dose instillation (Fig. 3B) when maximal cAMP accumulation was detected (Fig. 3C). Direct intrapulmonary application prevented PI3K γ MP from diffusing outside of the respiratory tract and from altering cAMP homeostasis in the heart (Fig. 3, A to C). No systemic side effects were observed after chronic exposure to PI3K γ MP, as evidenced by histopathological examination

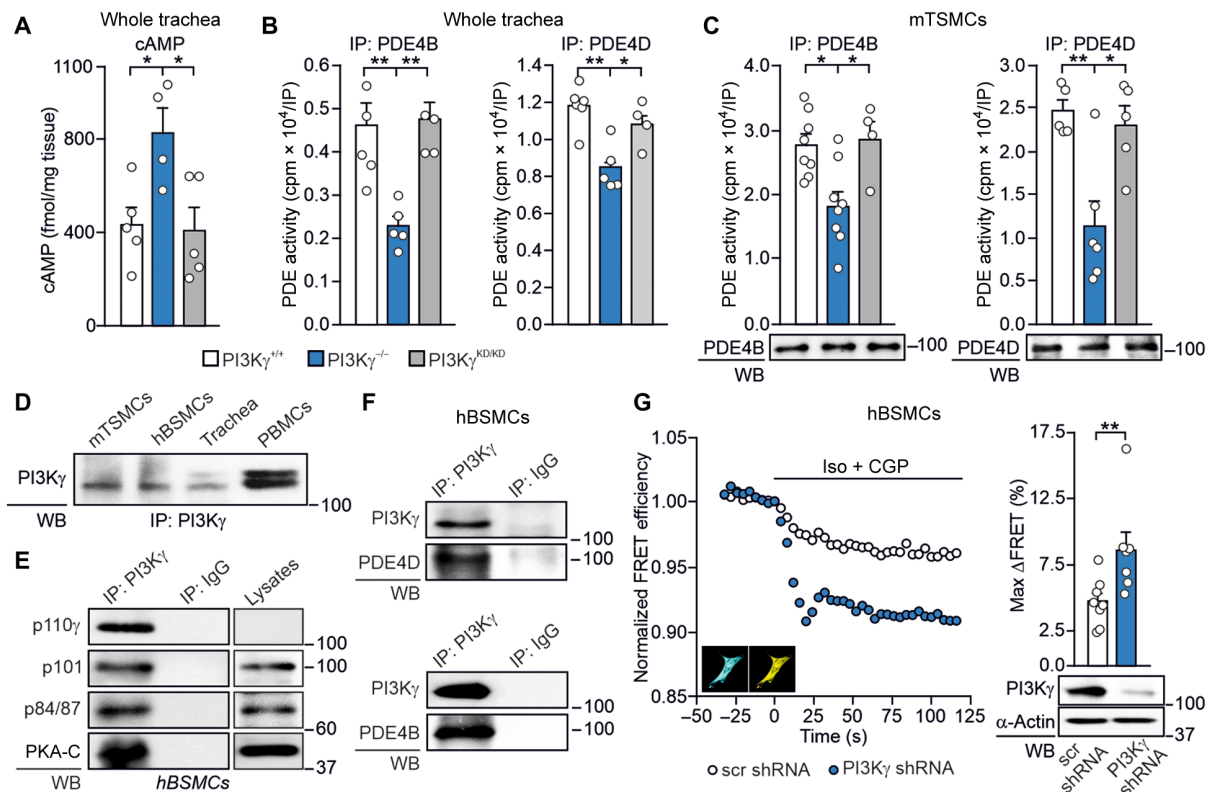


Fig. 1. PI3K γ decreases airway cAMP through kinase-dependent activation of PDE4B and PDE4D. (A) cAMP concentration in tracheas from PI3K $\gamma^{+/+}$ ($n = 5$), PI3K $\gamma^{KD/KD}$ ($n = 5$), and PI3K $\gamma^{-/-}$ ($n = 4$) mice. (B) Phosphodiesterase activity in PDE4B and PDE4D immunoprecipitates from PI3K $\gamma^{+/+}$ ($n = 5$ and $n = 6$), PI3K $\gamma^{KD/KD}$ ($n = 4$ and $n = 4$), and PI3K $\gamma^{-/-}$ ($n = 5$ and $n = 5$) tracheas. (C) Phosphodiesterase activity in PDE4B and PDE4D IP from PI3K $\gamma^{+/+}$ ($n = 8$ and $n = 5$), PI3K $\gamma^{KD/KD}$ ($n = 4$ and $n = 5$), and PI3K $\gamma^{-/-}$ ($n = 6$ and $n = 5$) independent cultures of murine tracheal smooth muscle cells (mTSMCs). Western blots (WBs) of representative IPs are shown. (D) Western blot of PI3K γ expression in mTSMCs, human bronchial smooth muscle cells (hBSMCs), and murine trachea. Peripheral blood mononuclear cells (PBMCs) are used as positive control. (E) Coimmunoprecipitation of PI3K γ catalytic subunit (p110 γ) with its relative adaptors (p101 and p84/87) and PKA catalytic subunit (PKA-C) in hBSMCs. (F) Coimmunoprecipitation of PI3K γ with PDE4B and PDE4D in hBSMCs. Immunoglobulin G (IgG) immunoprecipitation was used as control. In (D) to (F), representative Western blot images of $n = 4$ independent experiments are shown. (G) Representative fluorescence resonance energy transfer (FRET) (left) traces and (right) maximal FRET changes (max Δ FRET) of hBSMCs transfected with a FRET-based sensor for cytosolic cAMP (Epac2-cAMPs), together with either a short hairpin RNA (shRNA) against the *PIK3CG* gene encoding PI3K γ (PI3K γ shRNA; $n = 7$) or a scrambled shRNA (scr shRNA; $n = 9$) vector. β_2 -ARs were selectively activated by isoproterenol (Iso; 100 nM for 15 s) and the β_1 -AR-selective antagonist CGP-20712A (CGP; 100 nM). Insets: Representative cyan and yellow fluorescence protein images of hBSMCs expressing Epac2-cAMPs. n indicates the number of cells analyzed in $n = 3$ independent experiments. Representative Western blot of PI3K γ expression in hBSMCs 48 hours after transfection with the PI3K γ shRNA and scr shRNA is shown below the graph. In (A) to (C), * $P < 0.05$ and ** $P < 0.01$ by one-way ANOVA, followed by Bonferroni's post hoc test. In (G), ** $P < 0.01$ by Mann-Whitney test. Throughout, data are means \pm SEM.

of major organs (fig. S3A), body weight monitoring (fig. S3B), blood biochemical tests, and cardiac function analysis (tables S1 and S2). Furthermore, negligible immunogenicity was observed only after repeated systemic administration of the peptide in the presence of adjuvants (fig. S3C), whereas PI3K γ MP did not elicit any antibody response when applied locally (fig. S3D). Thus, inhalation of PI3K γ MP might be safely used to boost airway β_2 -AR/cAMP signaling in vivo.

PI3K γ MP induces airway relaxation in a mouse model of asthma

Next, we assessed ex vivo in mouse tracheal rings if the PI3K γ scaffold activity affected cAMP-dependent airway smooth muscle relaxation. Acetylcholine-induced contraction was lower in PI3K $\gamma^{-/-}$ tracheas than in PI3K $\gamma^{+/+}$ controls, whereas PI3K $\gamma^{KD/KD}$ rings exhibited normal tone (Fig. 4A). Similarly, carbachol-dependent contractility was 35% lower in PI3K $\gamma^{-/-}$ than in PI3K $\gamma^{+/+}$ and PI3K $\gamma^{KD/KD}$ samples

(Fig. 4B). Next, PI3K $\gamma^{+/+}$ and PI3K $\gamma^{-/-}$ rings were pretreated with the selective PDE4 inhibitor roflumilast before exposure to carbachol. PDE4 inhibition decreased the contraction of PI3K $\gamma^{+/+}$ rings to the values observed in PI3K $\gamma^{-/-}$ samples where the inhibitor was ineffective (Fig. 4C), thus confirming that the decreased contraction of PI3K $\gamma^{-/-}$ airways is causally linked to a reduction in PDE4 activity.

We then determined whether PI3K γ MP could phenocopy the reduced contractility observed in PI3K $\gamma^{-/-}$ airways. Lung resistance was assessed in healthy wt mice pretreated with an aerosol of PI3K γ MP, CP, or saline before exposure to increasing doses of the contracting agent methacholine (MCh). MCh triggered a dose-dependent increase in airway resistance that was lower in mice treated with PI3K γ MP than in animals exposed to CP (Fig. 4D). Next, we tested the ability of the peptide to promote airway relaxation in ovalbumin (OVA)-sensitized mice, a well-established model of asthma. Single-dose inhalation of PI3K γ MP significantly increased the amount of cAMP in lungs ($P = 0.0065$) and tracheas ($P = 0.0137$) (Fig. 4E) and

Downloaded from https://www.science.org at Universita Degli Studi Di Torino on March 31, 2022

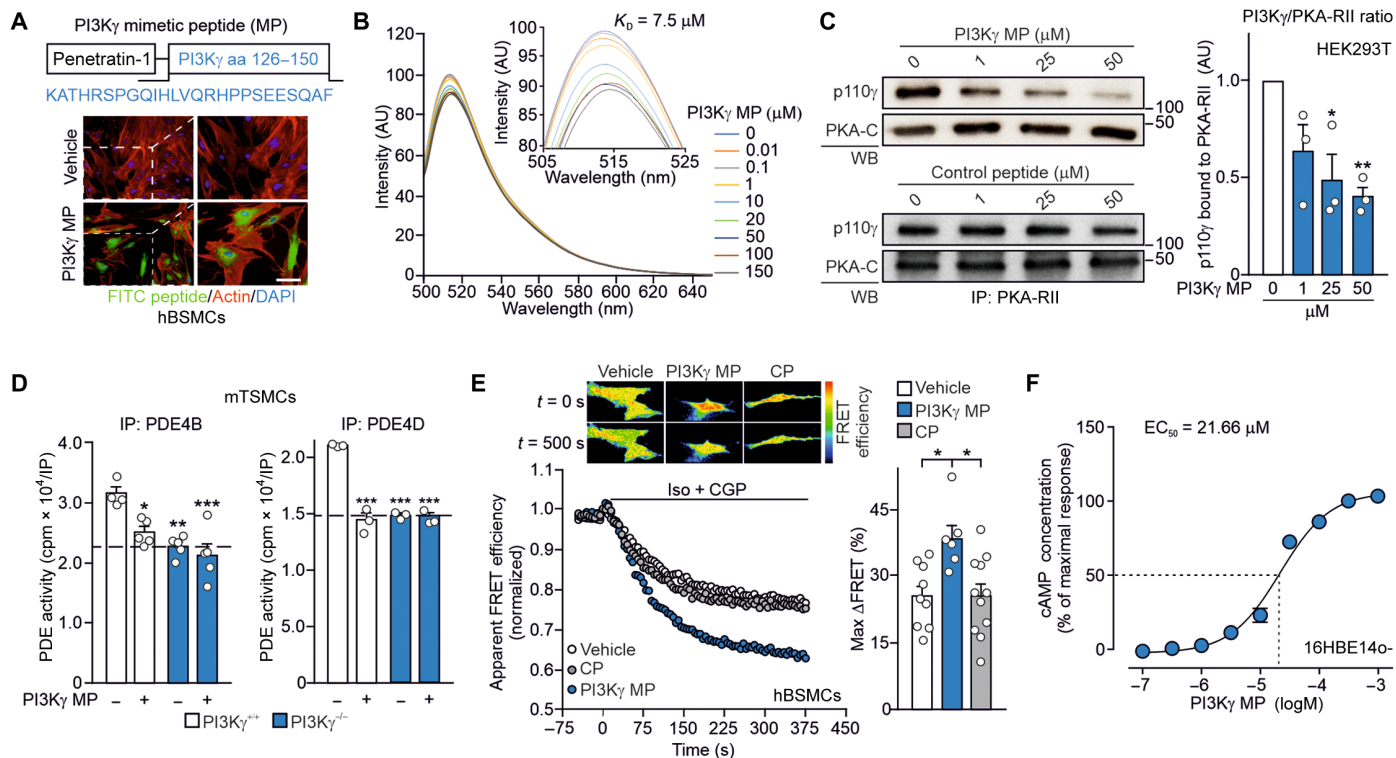


Fig. 2. PI3K γ MP enhances airway β_2 -AR/cAMP signaling in vitro. (A) Top: Schematic representation of the cell-permeable PI3K γ MP. The 126–150 region of PI3K γ was fused to the cell-penetrating peptide penetratin-1 (P1). Bottom: Intracellular fluorescence image of hBSMCs after 1-hour incubation with a FITC-labeled version of PI3K γ MP (50 μ M) or vehicle. Scale bar, 10 μ m. aa, amino acid; DAPI, 4',6-diamidino-2-phenylindole. (B) Steady-state emission spectra of recombinant fluorescein 5-maleimide-labeled PKA-R11 (PKA-F5M) in the presence of increasing concentrations of PI3K γ MP (0 to 150 μ M), revealing a dissociation constant for PI3K γ MP/PKA-R11 interaction of 7.5 μ M. AU, arbitrary units. (C) Coimmunoprecipitation of the catalytic subunit of PI3K γ (p110 γ) and PKA-R11 from human embryonic kidney 293T (HEK293T) cells expressing p110 γ and exposed to increasing doses of PI3K γ MP for 2 hours. Representative immunoblots (left) and relative quantification (right) of $n = 3$ independent experiments are shown. (D) PDE4B and PDE4D activity in PI3K $\gamma^{+/+}$ and PI3K $\gamma^{-/-}$ mTSMCs treated with either vehicle or PI3K γ MP (50 μ M) for 30 min. For PDE4B IP, PI3K $\gamma^{+/+}$ + vehicle, $n = 4$; PI3K $\gamma^{+/+}$ + PI3K γ MP, $n = 5$; PI3K $\gamma^{-/-}$ + vehicle, $n = 5$; and PI3K $\gamma^{-/-}$ + PI3K γ MP, $n = 5$ independent cultures. For PDE4D IP, $n = 3$ independent cultures in all groups. (E) Representative FRET traces (left) and maximal FRET changes (right) in hBSMCs expressing the indicator of cAMP using Epac (ICUE3) cAMP FRET sensor and pretreated for 30 min with vehicle ($n = 9$), 50 μ M PI3K γ MP ($n = 6$), or equimolar control peptide (CP) ($n = 11$) before activation of β_2 -adrenergic receptors (β_2 -ARs) with isoproterenol and the β_1 -AR antagonist CGP-20712A (Iso + CGP) (100 nM each). Insets show representative intensity-modulated pseudocolor images at $t = 0$ and 500 s after the addition of Iso + CGP. n indicates the number of cells analyzed in $n = 3$ independent experiments. (F) cAMP elevation in human bronchial epithelial (HBE) cells (16HBE140-) in response to increasing concentrations of PI3K γ MP (31.6 nM to 316 μ M range) for 30 min. The amount of cAMP was expressed as percentage of cAMP accumulation elicited by 100 μ M PI3K γ MP. $N = 6$ independent experiments. In (C) to (E), * $P < 0.05$, ** $P < 0.01$, and *** $P < 0.001$ by one-way ANOVA, followed by Bonferroni's post hoc test. In (F), nonlinear regression analysis was used. Throughout, data are means \pm SEM.

reduced MCh-induced bronchoconstriction, as evidenced by measurements of both tidal volume (Fig. 4F) and lung resistance (Fig. 4G). Thus, PI3K γ MP could alleviate bronchoconstriction associated with asthma via elevation of cAMP.

PI3K γ MP limits neutrophilic inflammation in a mouse model of asthma

Because cAMP-elevating agents have anti-inflammatory actions (3), we tested whether PI3K γ MP could relieve airway inflammation in OVA-sensitized mice. Peribronchial inflammation and mucin production were dampened in animals repeatedly exposed to PI3K γ MP (Fig. 5, A and B). Moreover, a significantly lower number of neutrophils was detected in the bronchoalveolar lavage fluid of PI3K γ MP-treated mice than in controls ($P = 0.0437$) (Fig. 5C), indicating that PI3K γ MP inhibits the neutrophilic inflammation associated with asthma. PI3K γ MP also inhibited chemoattractant-induced adhesion of human neutrophils to intercellular adhesion molecule-1 (ICAM-1) and ICAM-2 (fig. S4, A and B) by reducing lymphocyte

function-associated antigen 1 (LFA-1) activation (fig. S4C). PKA inhibition rescued neutrophil adhesion to ICAM-1, ICAM-2, and fibrinogen (Fig. 5, D to F) in the presence of PI3K γ MP, indicating that the impaired adhesion was dependent on PKA hyperactivation. In line with ICAM-1 controlling neutrophil recruitment to the airways, PI3K γ MP significantly reduced neutrophil chemotaxis to *N*-formyl-Met-Leu-Phe (fMLP) ($P < 0.0001$) via PKA activation (Fig. 5G) and the consequent inhibition of RhoA-mediated (Fig. 5H) LFA-1 triggering (13). Thus, PI3K γ MP could limit neutrophilic inflammation in asthma by dampening neutrophil adhesion and transmigration.

PI3K γ MP promotes cAMP-dependent activation of CFTR and chloride efflux in airway epithelial cells

Next, we tested whether PI3K γ MP could promote chloride (Cl $^-$) secretion via the cAMP-gated CFTR channel. PI3K γ was enriched at the apical membrane of 16HBE140- cells (fig. S5A) and coimmunoprecipitated with CFTR (fig. S5B). Fluorescence resonance energy transfer (FRET) analysis showed that, in response to forskolin (Fsk),

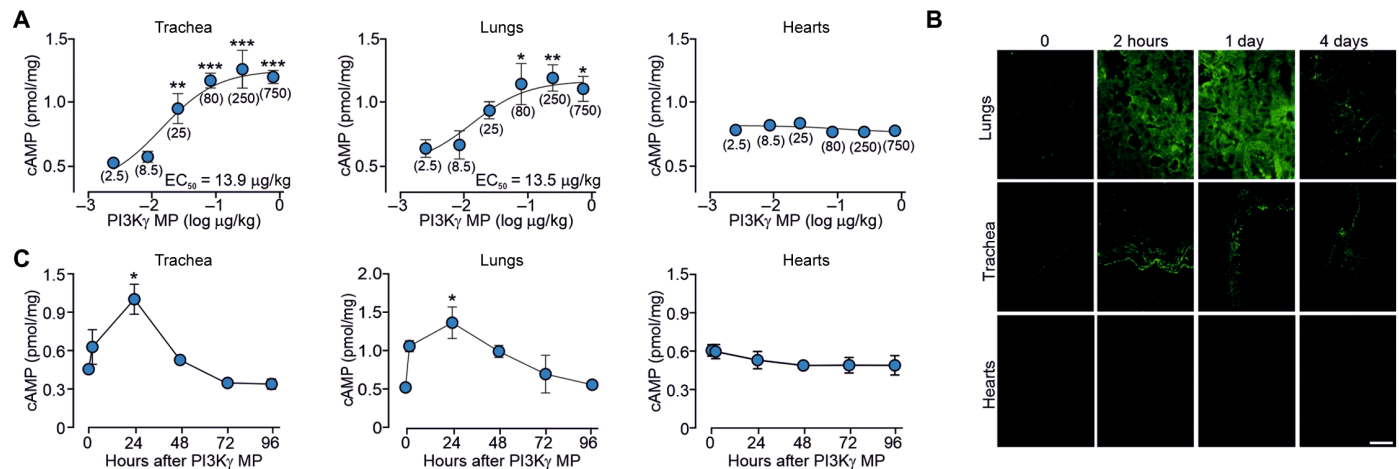


Fig. 3. PI3K γ MP elevates airway cAMP abundance in vivo in mice. (A) cAMP concentrations in tissues from BALB/c mice 24 hours after intratracheal instillation of different doses of PI3K γ MP (0 to 750 μ g/kg). Values in brackets indicate the dose of PI3K γ MP expressed as μ g/kg. The number of mice (n) ranged from three to nine per group. EC_{50} , median effective concentration. (B) Tissue distribution of a FITC-labeled version of PI3K γ MP at indicated time points after intratracheal instillation of 0.08 mg/kg (1.5 μ g) in BALB/c mice. Representative images of $n = 3$ experiments are shown. Scale bar, 50 μ m. (C) Amount of cAMP in tissues from mice treated as in (B). The number of mice (n) ranged from three to six per group. In (A), * $P < 0.05$, *** $P < 0.01$, and **** $P < 0.001$ by one-way ANOVA, followed by Bonferroni's post hoc test. In (C), * $P < 0.05$ by Kruskal-Wallis test, followed by Dunn's multiple comparison test. Throughout, data are means \pm SEM.

PI3K γ MP induced threefold higher subcortical membrane cAMP concentration than either CP or saline (Fig. 6A) while not affecting cytosolic cAMP responses (Fig. 6A).

To test whether PI3K γ MP could trigger CFTR gating, PKA-mediated phosphorylation of the channel was assessed by Western blot and found to be fivefold higher in 16HBE140- cells treated with PI3K γ MP than in cells exposed to either vehicle or CP (Fig. 6B). PI3K γ MP increased CFTR phosphorylation to a similar extent as rolipram, implying that PI3K γ MP affects the PDE4-mediated regulation of CFTR (14). To further characterize the CFTR phosphorylation elicited by PI3K γ MP, the phospho-occupancy of known PKA sites in the regulatory domain of the channel was analyzed by liquid chromatography-coupled tandem mass spectrometry in CF human bronchial epithelial (HBE) cells expressing a wt CFTR (wt-CFTR-CFBE410-) (15), treated with PI3K γ MP, CP, Fsk, or vehicle. Whereas Fsk-mediated adenylyl cyclase activation triggered the phosphorylation of most PKA sites, PI3K γ MP selectively increased the phospho-occupancy of S737 and, to a lesser extent, of S753 (Fig. 6C and fig. S6, A to C). In agreement with mass spectrometry results, the CFTR phosphorylation elicited by PI3K γ MP was completely abolished in cells expressing a CFTR mutant where the serine was replaced by alanine (Fig. 6D).

Because phosphorylation of S737 can lead to a ~25% increase in the open probability of CFTR (16), we anticipated that PI3K γ MP could activate Cl⁻ secretion. Measurement of short-circuit currents (I_{SC}) showed that acute application of PI3K γ MP to polarized wt-CFTR-CFBE410- monolayers induced a dose-dependent increase in CFTR conductance (fig. S7A), reaching up to either 30 or 45% of the maximal channel activation when applied either alone or in association with nanomolar doses of Fsk, respectively (fig. S7, A to C). Addition of the adenylyl cyclase inhibitor SQ22536 and the PKA blocker H89 after treatment with PI3K γ MP inhibited the increase in CFTR conductance elicited by the peptide (fig. S7D), confirming that PI3K γ MP activated CFTR through PKA.

I_{SC} measurements in primary HBE cells showed that PI3K γ MP, but not CP, induced a dose-dependent increase in CFTR currents

(Fig. 6E). No further elevation in I_{SC} was observed when rolipram was added to PI3K γ MP (Fig. 6E), confirming that the peptide inhibited the PDE4 pool associated to CFTR regulation (14). Boosting cAMP production with Fsk produced an additional increment of I_{SC} that was blocked by the CFTR inhibitor 172 (CFTR_{inh}-172) (Fig. 6E). Similarly, the nonhydrolysable cAMP analog CPT-cAMP further increased I_{SC} in addition to PI3K γ MP (fig. S8, A and B) but blocked the effect of the peptide on CFTR currents when applied as a pre-treatment (fig. S8, A to C), providing further evidence that PI3K γ MP activated the channel through cAMP and PKA.

Primary HBE cells express other cAMP/PKA-dependent ion channels and transporters that can indirectly influence CFTR activity by increasing the electrochemical driving force (17). In the presence of CFTR_{inh}-172, PI3K γ MP retained the ability to induce a transient increase in I_{SC} (fig. S8D), indicating the opening of Ca²⁺-activated Cl⁻ channels (CaCCs). Furthermore, the current decreased to baseline after application of clotrimazole (fig. S8D), an inhibitor of basolateral Ca²⁺-activated K⁺ channels, and bumetanide, an inhibitor of the Na-K-Cl cotransporter NKCC1 (fig. S8D), suggesting that the peptide could also promote luminal Cl⁻ secretion indirectly via these channels. To further evaluate the direct action of PI3K γ MP on CFTR currents, Ca²⁺ stores were first depleted with thapsigargin (fig. S8, E and F), and then, CaCCs were blocked using either a general CaCC inhibitor (fig. S8E) or an inhibitor targeting TMEM16A (fig. S8F), the major CaCC isoform in HBE cells. Without functional CaCCs, PI3K γ MP elicited a response that was fully abolished by CFTR_{inh}-172, confirming a direct activation of CFTR (fig. S8E). This observation was corroborated in rectal organoids, where CaCCs are not consistently expressed, and organoid swelling in response to Fsk [Fsk-induced swelling (FIS)] is CFTR dependent (18). PI3K γ MP potentiated by twofold the swelling of wt organoids elicited by a low dose of Fsk (2 μ M) priming cAMP production (Fig. 6F). As CFTR activation triggers water secretion, essential for proper mucus hydration and clearance (2), PI3K γ MP, but not CP, decreased intracellular water residence time, indicative of rapid water efflux, in cells expressing

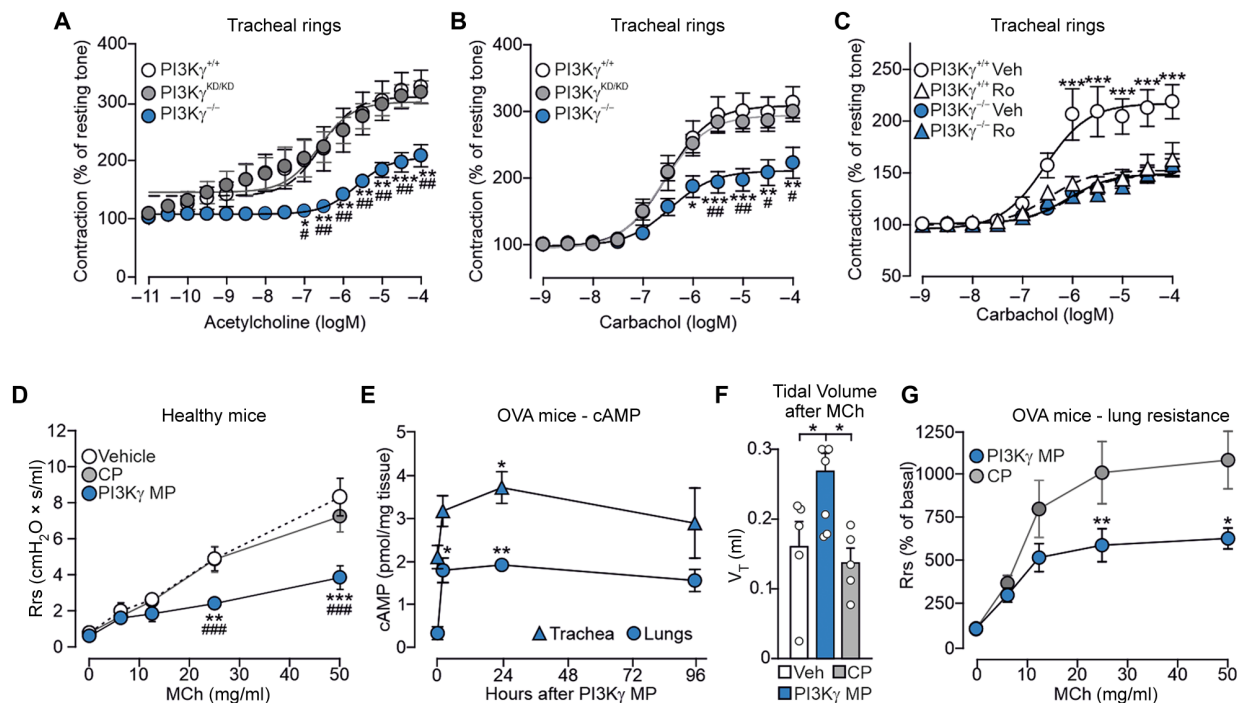


Fig. 4. PI3K γ MP promotes airway relaxation ex vivo and in vivo in a mouse model of asthma. (A and B) Cumulative contractile response of PI3K $\gamma^{+/+}$, PI3K $\gamma^{KD/KD}$, and PI3K $\gamma^{-/-}$ tracheal rings to increasing concentrations of acetylcholine (A) and carbachol (B). The developed tension is expressed as a percentage of the resting tone. In (A), PI3K $\gamma^{+/+}$, $n = 7$; PI3K $\gamma^{KD/KD}$, $n = 6$; and PI3K $\gamma^{-/-}$, $n = 5$ mice. In (B), PI3K $\gamma^{+/+}$, $n = 9$; PI3K $\gamma^{KD/KD}$, $n = 6$; and PI3K $\gamma^{-/-}$, $n = 5$ mice. (C) Cumulative contractile response to carbachol of PI3K $\gamma^{+/+}$ and PI3K $\gamma^{-/-}$ tracheal rings pretreated with either vehicle (Veh) or the PDE4 inhibitor roflumilast (Ro) (10 μ M) for 30 min. PI3K $\gamma^{+/+}$ + vehicle, $n = 10$; PI3K $\gamma^{+/+}$ + Ro, $n = 5$; PI3K $\gamma^{-/-}$ + vehicle, $n = 13$, and PI3K $\gamma^{-/-}$ + Ro, $n = 9$ mice. (D) Average lung resistance in healthy mice treated with vehicle ($n = 4$), 1.5 μ g of PI3K γ MP ($n = 4$), or equimolar amount of control peptide (CP) ($n = 5$) directly before exposure to increasing doses of the bronchoconstrictor methacholine (MCh). (E) cAMP concentrations in lungs and tracheas of ovalbumin (OVA)-sensitized mice at the indicated time points after intratracheal administration of PI3K γ MP (15 μ g). The number of mice (n) ranged from three to eight per group. (F) Tidal volume (V_T) of OVA-sensitized mice pretreated with Veh ($n = 5$), PI3K γ MP (15 μ g; $n = 6$), and CP (equimolar amounts; $n = 5$) and exposed to MCh (500 μ g/kg). (G) Average lung resistance (expressed as % of basal) in OVA-sensitized mice treated with 15 μ g of PI3K γ MP ($n = 9$) or equimolar amount of CP ($n = 10$) 30 min before MCh challenge. In (A) and (B), * $P < 0.05$, ** $P < 0.01$, and *** $P < 0.001$ versus PI3K $\gamma^{+/+}$ and # $P < 0.05$ and ### $P < 0.01$ versus PI3K $\gamma^{KD/KD}$ by two-way ANOVA, followed by Bonferroni's multiple comparisons test. In (C), ** $P < 0.01$ and *** $P < 0.001$ for PI3K $\gamma^{+/+}$ + vehicle versus all other groups by two-way ANOVA, followed by Bonferroni's multiple comparisons test. In (D), ** $P < 0.01$ and *** $P < 0.001$ versus vehicle and ### $P < 0.001$ versus CP by two-way ANOVA, followed by Bonferroni's post hoc test. In (E) and (F), * $P < 0.05$ and ** $P < 0.01$ by one-way ANOVA, followed by Bonferroni's post hoc test. In (G), * $P < 0.05$ and ** $P < 0.01$ between groups by two-way ANOVA, followed by Bonferroni's post hoc test. Throughout, data are means \pm SEM.

wt-CFTR (Fig. 6G). Hence, PI3K γ MP could induce Cl $^-$ and consequent water secretion in bronchial epithelial cells through a cAMP-dependent mechanism, coordinating direct CFTR gating with the elevation of the electrochemical driving force.

PI3K γ MP enhances the therapeutic effects of CFTR modulators in CF in vitro models

Next, we tested whether PI3K γ MP could rescue the function of the most common CF-causing CFTR mutant (F508del-CFTR). F508del-CFTR exhibits multiple molecular defects that require the combined use of correctors (VX-809/lumacaftor, VX-661/tezacaftor, or VX-445/elexacaftor) and a potentiator (VX-770/ivacaftor) to restore the plasma membrane localization and channel gating, respectively (2). In the presence of the corrector VX-809, PI3K γ MP enhanced subcortical cAMP concentrations by 35% in F508del-CFTR-CFBE41o- cells (Fig. 7A). Furthermore, primary HBE cells from a patient homozygous for the F508del mutation, treated with the first-generation combination of VX-809 and VX-770, showed a fivefold increase in I_{SC} when PI3K γ MP was given after acute administration of VX-770 (Fig. 7B). Similar results were obtained in

F508del/F508del HBE cells from a second donor, with the exception that in these cells, PI3K γ MP, added in addition to VX-770, stimulated a biphasic response, with a first I_{SC} peak that indicated CaCC activation, followed by a plateau phase corresponding to CFTR $_{inh-172}$ -sensitive CFTR-mediated currents (Fig. 7C and fig. S9, A to D). In agreement with a coordinated action of the peptide on CFTR currents and the electrochemical driving force, I_{SC} was completely abolished by sequential application of CFTR $_{inh-172}$, clotrimazole, and bumetanide (fig. S9, A to C). The synergy between the CFTR potentiator VX-770 and PI3K γ MP was further supported by FIS assays in intestinal organoids. The effect of the peptide was first assessed in organoids derived from compound heterozygotes bearing the F508del allele and the residual function mutation D1152H. After correction with VX-809, organoid size was increased by 50% in the group pretreated with PI3K γ MP before stimulation with VX-770 and Fsk (Fig. 7D), and CFTR $_{inh-172}$ prevented this effect (Fig. 7D). In F508del/F508del organoids under chronic treatment with VX-809 and VX-770, where their interaction reduces correction efficacy (19), PI3K γ MP dose-dependently increased organoid size up to 6.5-fold the volume of controls (Fig. 7E). The maximal synergy between the

Downloaded from https://www.science.org at Universita Degli Studi Di Torino on March 31, 2022

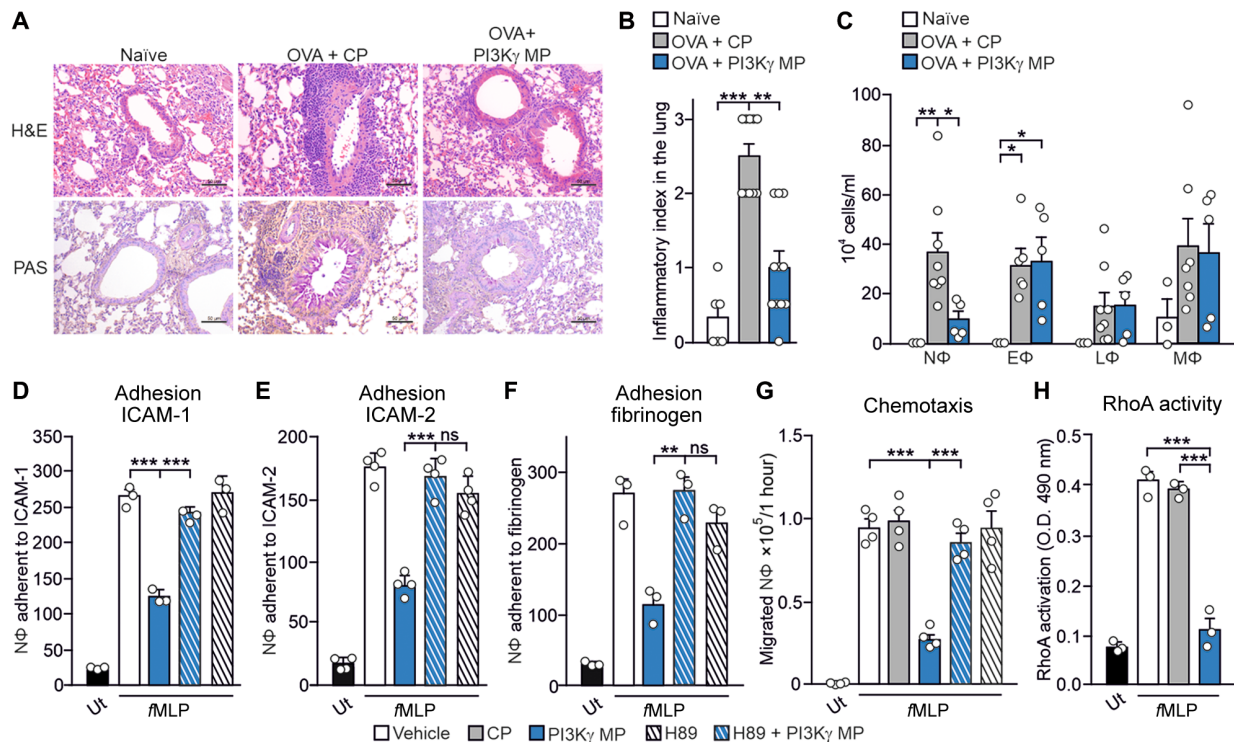


Fig. 5. PI3K γ MP limits neutrophilic lung inflammation in asthmatic mice. (A) Representative images of hematoxylin-eosin (H&E) (top) and periodic acid–Schiff's reagent (PAS) (bottom) staining of lung sections of naïve and OVA-sensitized mice, pretreated with PI3K γ MP (25 μ M) or CP (equimolar amount), before each intranasal OVA administration (days 14, 25, 26, and 27 of the OVA-sensitization protocol). Scale bars, 50 μ m. (B) Semiquantitative analysis of peribronchial inflammation in lung sections as shown in (A). Naïve, $n=6$; OVA + CP, $n=8$; and OVA + PI3K γ MP, $n=5$ mice. (C) Number of neutrophils (N Φ), eosinophils (E Φ), lymphocytes (L Φ), and macrophages (M Φ) in the bronchoalveolar lavage fluid of mice treated as in (A). Naïve, $n=3$; OVA + CP, $n=8$; and OVA + PI3K γ MP, $n=5$ animals. (D to F) β MLP-induced adhesion to ICAM-1 (D), ICAM-2 (E), and fibrinogen (F) of human neutrophils pretreated or not with the PKA inhibitor H89 (200 nM for 30 min) before exposure to vehicle or PI3K γ MP (50 μ M for 1 hour). Static adhesion was induced with 25 nM β MLP for 1 min. Average numbers of adherent cells/0.2 mm² are shown. In (D) and (F), $n=3$ in all groups; in (E), $n=4$ in all groups. (G) β MLP-triggered chemotaxis of human neutrophils treated with vehicle, CP (50 μ M), or PI3K γ MP (50 μ M) for 1 hour, without or with pretreatment with the PKA inhibitor H89 (200 nM for 30 min). $n=4$ in all groups. (H) β MLP-induced RhoA activity in human neutrophils treated with vehicle, CP (50 μ M), or PI3K γ MP (50 μ M). $n=3$ in all groups. In (B), $**P < 0.01$ and $***P < 0.001$ by Kruskal-Wallis test, followed by Dunn's multiple comparison test. In (C) to (H), $*P < 0.05$, $**P < 0.01$, and $***P < 0.001$ by one-way ANOVA, followed by Bonferroni's post hoc test. O.D., optical density. ns, not significant; Ut, untreated.

peptide and CFTR modulators was observed at a low nonsaturating dose of Fsk (0.051 μ M), which was expected to minimally increase the amount of cAMP and which was almost ineffective in inducing swelling in the control VX-770 + VX-809 group.

Last, we assessed the ability of PI3K γ MP to enhance the therapeutic effects of the recent triple combination elexacaftor/tezacaftor/ivacaftor (ETI) (VX-445 + VX-661 + VX-770) in F508del/F508del HBE cells from two different donors with CF. VX-770-mediated Cl⁻ currents were 40% higher in cells treated chronically with VX-661 + VX-445 together with PI3K γ MP than in controls exposed to correctors alone (Fig. 8, A to C, and fig. S9E). In both cases, CPT-cAMP further increased Cl⁻ currents, which were inhibited by CFTR_{inh}-172, further demonstrating that Cl⁻ secretion was CFTR dependent. These data thus suggest the use of PI3K γ MP to increase the efficacy of CFTR modulators and to provide bronchodilator and anti-inflammatory activities, potentially beneficial to CF and other diseases like COPD and asthma.

DISCUSSION

Our results establish that targeting the PKA-anchoring function of PI3K γ with an MP allows therapeutic manipulation of β_2 -AR/cAMP

signaling in multiple cell types participating to the pathogenesis of chronic obstructive airway diseases (fig. S10). These findings are consistent with a model where PI3K γ acts as a scaffold protein for PKA (AKAP) in a complex containing the PKA-dependent phosphodiesterase PDE4 (7). The pharmacological actions of PI3K γ MP stem from its ability to displace PKA from the PI3K γ complex, thereby preventing PKA-mediated stimulation of a pool of PDE4 that is responsible for lowering the amount of cAMP close to neighboring distinct PKA-containing complexes, including those regulating CFTR gating (14).

Our finding that PI3K γ MP fails to increase cAMP in PI3K γ -deficient cells demonstrates that the peptide inhibits uniquely PI3K γ -dependent PDEs and does so without disturbing other AKAP-PKA complexes. This is supported by our previous findings showing that the PKA-binding sequence of the peptide diverges from that of classical AKAPs (10).

Although the AKAP function of PI3K γ has been previously linked to cAMP modulation in the heart (9, 10) and in vascular smooth muscles (20), the role and the pathophysiological relevance of PI3K γ noncatalytic activity outside the cardiovascular system has remained elusive. The present study identified the scaffold function

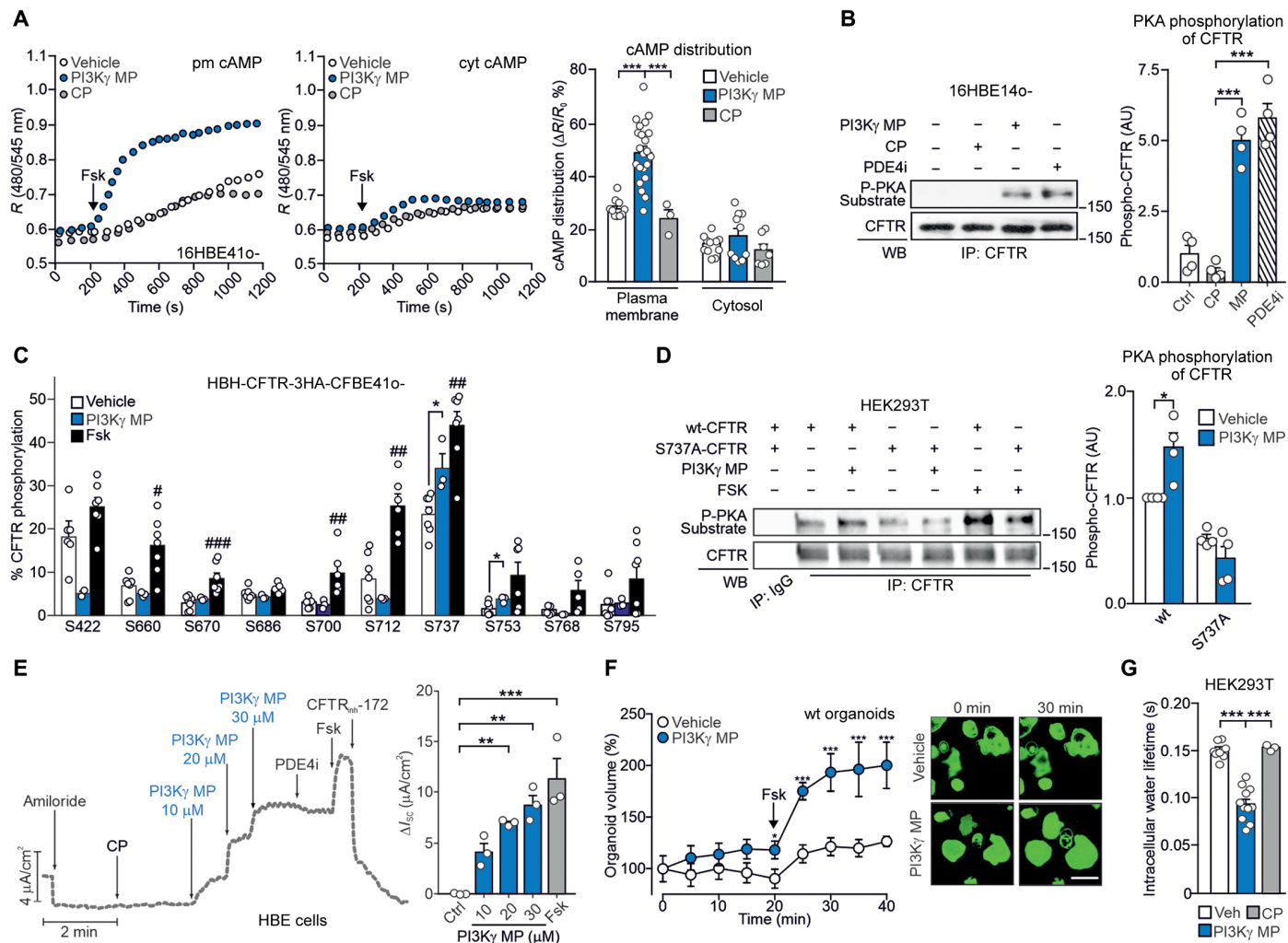


Fig. 6. PI3K γ MP promotes cAMP-dependent gating of CFTR. (A) Representative FRET traces (left) and maximal FRET changes (right) in HBE cells (16HBE140o) expressing the FRET probe for either plasma membrane (pm cAMP) or cytosolic cAMP (cyt cAMP). Cells were preincubated with vehicle, PI3K γ MP (25 μ M), or control peptide (CP) (25 μ M) before treatment with 1 μ M forskolin (Fsk). *R* is the normalized 480 nm/545 nm emission ratio calculated at indicated time points. *n* indicates the number of cells from *n* = 3 independent experiments. vehicle, *n* = 10 and *n* = 12; PI3K γ MP, *n* = 22 and *n* = 11; and CP *n* = 3 and *n* = 7 for pm cAMP and cyt cAMP, respectively. (B) Representative Western blot (left) and relative quantification (right) of PKA-mediated phosphorylation of CFTR in 16HBE140o cells treated with vehicle, CP (25 μ M), PI3K γ MP (25 μ M), and the PDE4 inhibitor rolipram (PDE4i) (10 μ M) for 30 min. CFTR was immunoprecipitated, and PKA-dependent phosphorylation was detected in IP pellets by immunoblotting with a PKA substrate antibody. *n* = 4 independent experiments. (C) Relative phosphorylation (%) or phospho-occupancy of identified PKA sites of CFTR in wt-CFTR-CFBE41o-expressing HBH-CFTR-3HA treated with vehicle [dimethyl sulfoxide (DMSO); *n* = 7], PI3K γ MP (25 μ M for 1 hour, *n* = 3), and Fsk (10 μ M for 10 min, *n* = 7). *n* is the number of biological replicates from *n* = 3 independent experiments. The phospho-occupancy or the percent of relative phosphorylation of each site was calculated as a ratio of all phosphorylated and unphosphorylated peptides that contained a given phosphorylation site [% phosphorylation of site A = (area of peptides phosphorylated at site A/sum of areas of all peptides carrying site A) as described in Materials and Methods]. Representative fragmentation spectra from each identified phosphorylation site and representative chromatograms from S737-containing peptides in their unphosphorylated and phosphorylated form are provided in fig. S6. (D) Representative Western blot (left) and relative quantification (right) of PKA-mediated phosphorylation of CFTR in HEK293T cells expressing either wt- or S737A-CFTR and exposed to vehicle, PI3K γ MP (25 μ M, 1 hour), or Fsk (10 μ M, 10 min). *n* = 4 independent experiments. (E) Left: Representative trace of short-circuit currents (*I*_{sc}) measured in Ussing chambers in primary normal HBE cells cultured at the air-liquid interface (ALI). The following treatments were applied at the indicated times: epithelial sodium channel inhibitor amiloride (10 μ M), CP (30 μ M), PI3K γ MP (10 to 30 μ M), PDE4 inhibitor rolipram (PDE4i) (10 μ M), Fsk (10 μ M), and CFTR inhibitor 172 (CFTR_{inh}-172) (20 μ M). Right: Average current variations in response to the indicated treatments. *n* = 3 biological replicates from the same donor. (F) Normalized swelling curves (left) and representative confocal images (right) of Fsk-stimulated calcein green-labeled wt organoids pre-incubated with PI3K γ MP (25 μ M) or vehicle for 20 min. Fsk was used at 2 μ M. Scale bar, 100 μ m. Vehicle, *n* = 25 and PI3K γ MP, *n* = 28 organoids from *n* = 3 independent experiments. (G) Water residence time (τ_{in}) determined by ¹H nuclear magnetic resonance relaxometry (as described in the Supplementary Materials) in HEK293T cells transfected with wt-CFTR and treated with vehicle (DMSO; *n* = 8), CP (25 μ M; *n* = 3), and PI3K γ MP (25 μ M; *n* = 11). *n* indicates the number of biological replicates in *n* = 3 independent experiments. In (A), (B), (D), (E), and (G), **P* < 0.05, ***P* < 0.01, and ****P* < 0.001 by one-way ANOVA, followed by Bonferroni's post hoc test. In (C), unpaired *t* tests, followed by Holm-Sidak's multiple comparisons test were performed on each phosphorylation site between two different treatment conditions. #*P* < 0.05, ##*P* < 0.01, and ###*P* < 0.001 Fsk versus vehicle and **P* < 0.05 PI3K γ MP versus vehicle. (F) **P* < 0.05 and ****P* < 0.001 by two-way ANOVA followed by Bonferroni's multiple comparisons test. Throughout, data are means \pm SEM.

Downloaded from https://www.science.org at Universita Degli Studi Di Torino on March 31, 2022

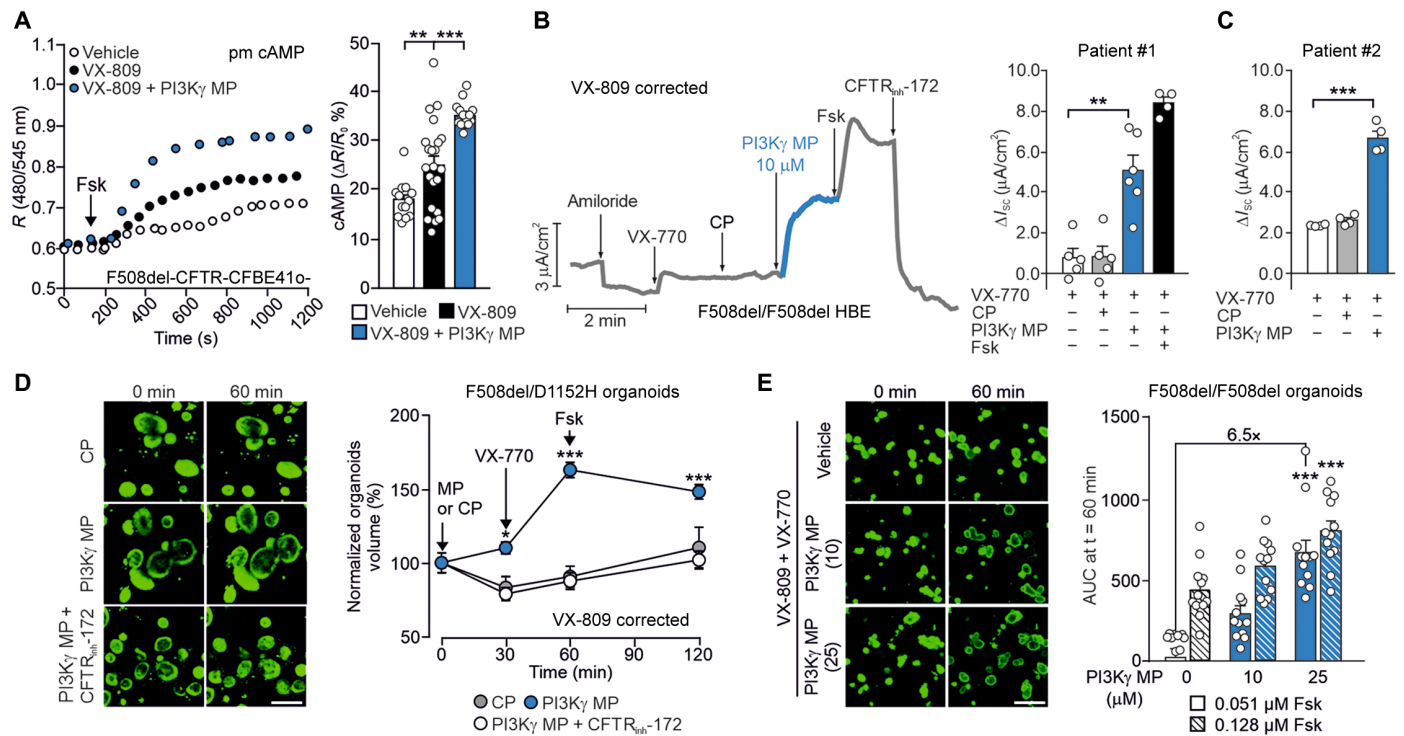


Fig. 7. PI3K γ MP potentiates the therapeutic effects of CFTR modulators in CF in vitro models. (A) Representative FRET traces (left) and maximal FRET changes (right) in CFBE41o- cells overexpressing F508del-CFTR and the plasma membrane-targeted FRET probe for cAMP (pm cAMP). Cells were preincubated with vehicle, the CFTR corrector VX-809 (5 μ M) alone, or together with PI3K γ MP (25 μ M) before treatment with 1 μ M Fsk. *R* is the normalized 480 nm/545 nm emission ratio calculated at indicated time points. Vehicle, *n* = 12; VX-809, *n* = 22; and VX-809 + PI3K γ MP, *n* = 16, where *n* is the number of cells from *n* = 3 independent experiments. (B) Left: Representative trace of short-circuit currents (*I*_{sc}) in primary HBE cells from a donor with CF (patient #1) homozygous for the F508del mutation (F508del/F508del HBE) and grown at the ALI. Cells were corrected with VX-809 for 48 hours (5 μ M) and then exposed to the following drugs at the indicated times: amiloride (100 μ M), CP (10 μ M), PI3K γ MP (10 μ M), Fsk (10 μ M), VX-770 (1 μ M), and CFTR_{inh}-172 (10 μ M). Right: Average total current variation in response to VX-770 (1 μ M), CP (25 μ M), and Fsk (10 μ M) of *n* = 4 technical replicates of the same donor. (C) Average total current variation in response to VX-770 (1 μ M), CP (25 μ M), and PI3K γ MP (25 μ M) in F508del/F508del HBE cells from a second donor with CF (patient #2) grown at ALI and precorrected with VX-809 for 48 hours (5 μ M). *n* = 4 technical replicates of the same donor. Representative *I*_{sc} traces are provided in fig. S9 (A to C). (D) Representative confocal images and quantification of Fsk-induced swelling (FIS) of calcein green-labeled rectal organoids from a patient carrying compound CF F508del and D1152H mutations (F508del/D1152H). Organoids were corrected with VX-809 (3 μ M) for 24 hours, incubated with calcein green (3 μ M) for 30 min, and exposed to either PI3K γ MP or CP (both 25 μ M) for 30 min before stimulation with Fsk (2 μ M). Organoid response was measured as a percentage change in volume at different time points after addition of Fsk (*t* = 30, *t* = 60, and *t* = 120 min) compared to the volume at *t* = 0. *n* = 15 to 34 organoids from one donor in *n* = 2 independent experiments. Scale bar, 200 μ m. (E) FIS responses (right) and representative confocal images (left) of calcein green-labeled rectal organoids from a CF patient homozygous for the F508del mutation (F508del/F508del). Organoids were preincubated with the CFTR corrector VX-809 (3 μ M) and the CFTR potentiator VX-770 (3 μ M) for 24 hours before exposure to two different concentrations of Fsk (0.51 and 0.128 μ M) and PI3K γ MP (10 and 5 μ M). The peptide was added to the organoids together with Fsk. Organoid response was measured as area under the curve of relative size increase of organoids after 60 min Fsk stimulation, *t* = 0 min: baseline of 100%. *n* = 12 organoids per group analyzed in *n* = 2 independent cultures from *n* = 2 different donors. Scale bar, 200 μ m. In (A) to (C), *****P* < 0.01** and ******P* < 0.001** by one-way ANOVA, followed by Bonferroni's post hoc test. In (D), ****P* < 0.05** and ******P* < 0.001** by two-way ANOVA, followed by Bonferroni's post hoc test. In (E), ******P* < 0.001** by Kruskal-Wallis test, followed by Dunn's multiple comparisons test. Throughout, data are means \pm SEM.

of PI3K γ as a key negative regulator of a discrete cAMP/PKA microdomain in different cell subsets of the airways, including epithelial, smooth muscle, and immune cells. Like in cardiomyocytes (9), in airway cells PI3K γ -mediated reduction of cAMP is spatially confined to compartments that contain β_2 -ARs, key pharmacological targets for respiratory diseases. Although the effects of PI3K γ MP might be attained with the use of β_2 -AR agonists, these drugs suffer from efficacy and tolerability concerns linked to tachyphylaxis and unwanted pharmacological effects outside the lungs. Unlike β_2 -AR agonists, PI3K γ MP acts through a distinct mechanism with at least two advantages. First, PI3K γ MP amplifies β_2 -AR/cAMP responses by impinging on cAMP degradation rather than on β_2 -AR activation, thus avoiding receptor desensitization, which, in the long run, is a

major cause of reduced efficacy. Second, being an inhaled peptide of 5 kDa, PI3K γ MP boosts lung cAMP without reaching other tissues where cAMP elevation would not be desirable, such as in the heart (9).

In addition, the local action of the peptide provides an added value over other cAMP-elevating agents, such as the classical small-molecule PDE4 inhibitors, like roflumilast, that easily diffuse outside the lungs and trigger undesired brain and cardiac effects (8). In addition, small-molecule PDE4 inhibitors lead to indiscriminate inhibition of all four different PDE4 subtypes (PDE4A, PDE4B, PDE4C, and PDE4D), potentially causing further side effects. PI3K γ MP blocked selective PDE4 subtypes with a prominent role in the lungs, such as PDE4B and PDE4D (21), with high isoform and compartment selectivity.

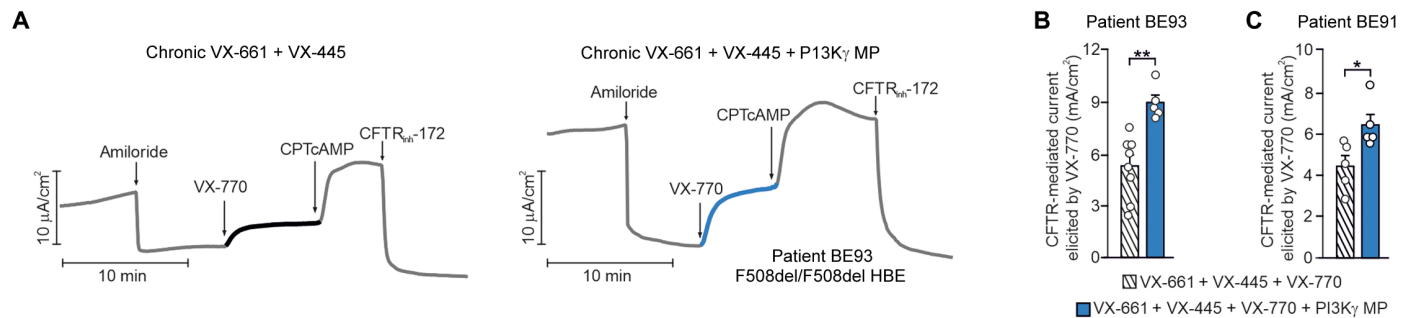


Fig. 8. PI3K γ MP enhances the effect of ETI in primary F508del/F508del HBE cells. (A) Representative traces of I_{SC} in primary HBE from a donor with CF (patient BE93) homozygous for the F508del mutation (F508del/F508del HBE) and grown at the ALI. Cells were corrected for 24 hours with VX-661 and VX-445 alone (10 μ M + 3 μ M) or together with PI3K γ MP (10 μ M) before exposure at the indicated time to the following drugs: amiloride (100 μ M), VX-770 (1 μ M), CPT-cAMP (100 μ M), and CFTR_{inh}-172 (10 μ M). (B) Average total current variation in response to VX-770 (1 μ M) from $n = 5$ to 8 technical replicates of donor BE93. (C) Average total current variation in response to VX-770 (1 μ M) from $n = 5$ technical replicates of a second F508del/F508del donor (patient BE91). Representative I_{SC} traces are provided in fig. S9E. Throughout, * $P < 0.05$ and ** $P < 0.001$ and by Student's t test. Data are means \pm SEM.

Consistent with the prorelaxing action of cAMP, PI3K γ MP demonstrated prominent bronchodilator effects *in vivo* in healthy and asthmatic mice, which could be explained by enhanced β_2 -AR/cAMP signaling, secondary to PDE4 inhibition in airway smooth muscle cells. Although the bronchorelaxant action of β_2 -AR agonists, such as salbutamol and formoterol, is well established, conflicting findings have been reported for PDE4 inhibitors (21). Our observation that roflumilast blunts PI3K γ -dependent contractility of tracheal rings confirms a role for PDE4 in regulating airway smooth muscle tone. This view agrees with previous reports of reduced airway smooth muscle contractility in *Pde4d* knockout mice (22) and of enhanced β_2 -AR-stimulated cAMP accumulation in *PDE4D5* knockdown human smooth muscle cells (23).

PDE4 is also enriched in immune cells, and PDE4 inhibitors have demonstrated anti-inflammatory properties (7, 21). The finding that PI3K γ MP specifically inhibited neutrophil recruitment suggests that this peptide might be effective in hard-to-treat chronic airway disease subtypes with neutrophilic inflammation, such as corticosteroid-insensitive neutrophilic asthma (24), as well as COPD and CF (2, 25). Similar to standard anti-inflammatory drugs, such as inhaled corticosteroids, PI3K γ MP might increase the risk of respiratory infections, requiring antibiotic therapy. This is particularly relevant to patients with CF who already suffer from infections causing lung function decline and, ultimately, mortality (2). A limitation of our study is that the effects of PI3K γ MP were not tested in infection models. Hence, although genetic and pharmacologic PDE4 inhibition appear safe in pulmonary infections (26), future studies are required to define whether PI3K γ MP affects host defense.

Another effect of targeting PDE4 is the cAMP/PKA-dependent gating of the CFTR channel, increasing airway surface liquid and facilitating mucus clearance (27). CFTR functional defects and mucus stasis can be observed in patients with COPD and certain forms of asthma (28) but are critical in CF (2). Previous reports identified PDE4D as a negative regulator of the cAMP/PKA-dependent activation of wt-CFTR in bronchial epithelial cells, highlighting the potential of PDE4 inhibitors to stimulate the channel (14, 29). Our study pinpoints PI3K γ as a key AKAP orchestrating cAMP-mediated signal transduction in a microdomain involving β_2 -ARs, PDE4D, and CFTR. Accordingly, whereas a generalized cAMP elevation induced by Fsk correlated with the phosphorylation of most of CFTR

phospho-sites, PI3K γ MP triggered local cAMP elevation, resulting in the selective phosphorylation of S737. Although S737 phosphorylation might have contrasting effects on CFTR gating (16, 30), this likely depends on contextual modifications of other phosphorylation sites (31), and our observations indicate that PI3K γ MP-mediated phosphorylation of S737 triggers the same activity observed after reintroduction of S737 in a PKA-insensitive CFTR mutant (16). PI3K γ MP contributes to Cl^- secretion not only through a direct action on CFTR but also by engaging Ca^{2+} -activated Cl^- channels and basolateral, clotrimazole-sensitive Ca^{2+} -activated K^+ channels increasing the electrochemical driving force (17). Hence, PI3K γ MP coordinates different mechanisms culminating in Cl^- secretion, provided that sufficient functional CFTR is appropriately located at the plasma membrane.

In CF, the most common CFTR mutation (F508del) leads to the intracellular retention of the channel (2). The function of F508del-CFTR can be improved by the combined administration of correctors and potentiators, which enable the plasma membrane exposure and facilitate PKA-dependent gating of the mutant channel, respectively (2, 32). In agreement, the efficacy of the potentiator VX-770 depends on concomitant cAMP/PKA phosphorylation of the channel (33). Although Fsk has been extensively used to elevate cAMP in the preclinical testing of all CFTR modulators, PI3K γ MP ensured a more physiological and compartment-restricted increase in cAMP in the vicinity of CFTR that maximized the action of all combinations, including both lumacaftor/ivacaftor and ETI. Despite the improvement in lung function achieved with ETI (2), rescue of CFTR activity does not reach more than 60% of physiological values (34, 35). Our observation that the peptide can almost double the gating of the F508del-CFTR mutant after correction and potentiation with ETI suggests that enhancing PKA-mediated CFTR phosphorylation might represent an avenue for reinstating F508del-CFTR activity close to 100% of wt function, a condition potentially matching that of healthy carriers of CF mutations (34). Our initial preclinical toxicology studies in mice have shown that the inhaled PI3K γ MP remains confined in the lungs and is tolerable, but additional investigations in other animal models are awaited to corroborate the ability of the aerosolized peptide to overcome the mucus barrier imposed by CF (36). Nonetheless, treatment with ETI is associated with a substantial improvement in mucus mobilization (37) and could thus facilitate the combined action of PI3K γ MP.

Together, this study highlights the therapeutic potential of increasing cAMP concentrations in a compartmentalized manner. With its pharmacological properties, PI3K γ MP might be useful for the treatment of airway diseases including asthma and COPD, where cAMP-elevating agents with broncho-relaxant properties are highly desirable. In addition, by inhibiting PDE4, PI3K γ MP may exert a selective activity on neutrophil adhesion and pulmonary recruitment. Last, PI3K γ MP might be used in CF where, despite the success of currently approved modulators, treatments allowing patients a normal life span are still lacking.

MATERIALS AND METHODS

Study design

We tested the hypothesis that targeting the scaffold function of PI3K γ could trigger local cAMP elevation in the lungs and could reduce airway smooth constriction, pulmonary inflammation, and mucus stasis in chronic respiratory diseases without incurring unwanted systemic side effects. We devised a cell-penetrating peptide disturbing the AKAP function of PI3K γ (PI3K γ MP), and we tested its ability to induce compartmentalized cAMP responses in vitro in hBSMCs and epithelial (16HBE14o-) cells, as well as in vivo after intratracheal instillation in mice. Bronchodilator and anti-inflammatory activities of PI3K γ MP were studied in vivo in a mouse model of asthma (OVA-sensitized mice). Effects on CFTR activity were studied in primary HBE cells and intestinal organoids from healthy controls and donors with CF through I_{sc} measurements and FIS assays, respectively.

The sample size for each experiment is included in the figure legends. For mouse studies, females and males of 8 to 12 weeks of age were used and randomly assigned to the experimental groups. Experiments were approved by the animal ethical committee of the University of Torino and by the Italian Ministry of Health (authorization no. 757/2016-PR). The number of mice in each group was determined by power calculations based on previous experience with the model system and is defined in the respective figure legends. For in vitro experiments using immortalized cell lines, at least three independent experiments were performed. For in vitro studies in cells and organoids derived from human subjects, the results of at least $n = 2$ independent cultures from $n = 2$ different donors are provided. Informed consent was obtained from all participating subjects, and all studies were ethically approved. All experiments were conducted by blinded researchers. When outliers were identified, they were excluded from analysis if justified based on confirmed technical failure in parameter acquisition. Further details can be found in relevant sections within the Supplementary Materials and Methods.

Animals

PI3K γ -deficient mice (PI3K $\gamma^{-/-}$) and knock-in mice with catalytically inactive PI3K γ (PI3K $\gamma^{KD/KD}$) were described previously (38, 39). Mutant mice were back-crossed with C57Bl/6j mice for 15 generations to inbreed the genetic background, and C57Bl/6j mice were used as controls (PI3K $\gamma^{+/+}$). For asthma studies, wt BALB/c females were used. Mice used in all experiments were 8 to 12 weeks of age. Mice were group-housed, provided free access to standard chow and water in a controlled facility providing a 12-hour light/12-hour dark cycle, and were used according to institutional animal welfare guidelines and legislation, approved by the local Animal Ethics

Committee. All animal experiments were approved by the animal ethical committee of the University of Torino and by the Italian Ministry of Health (authorization no. 757/2016-PR).

Human material

Approval for primary bronchial epithelial cells and organoids cultures was obtained by the different local ethics committees (University of California San Francisco, Istituto Giannina Gaslini, the University of North Carolina at Chapel Hill, University of Verona, and University Medical Center Utrecht), and informed consent was obtained from all participating subjects.

Statistical analysis

Prism software (GraphPad Software Inc.) was used for statistical analysis. Data are presented as scatter plots with bars (means \pm SEM). Raw data were first analyzed to confirm their normal distribution via the Shapiro-Wilk test and then analyzed by unpaired Student's t test, one-way analysis of variance (ANOVA), or two-way ANOVA. Bonferroni correction (one-way and two-way ANOVA) was applied to correct for multiple comparisons. In the absence of a normal distribution, nonparametric Kruskal-Wallis or Mann-Whitney tests were used, followed by Dunn's correction for multiple comparisons if appropriate. $P < 0.05$ was considered significant.

SUPPLEMENTARY MATERIALS

www.science.org/doi/10.1126/scitranslmed.abl6328

Materials and Methods

Figs. S1 to S10

Tables S1 and S2

Data files S1 and S2

MDAR reproducibility checklist

References (40–60)

[View/request a protocol for this paper from Bio-protocol](#)

REFERENCES AND NOTES

1. B. R. Celli, J. A. Wedzicha, Update on clinical aspects of chronic obstructive pulmonary disease. *N. Engl. J. Med.* **381**, 1257–1266 (2019).
2. M. Shteinberg, I. J. Haq, D. Polineni, J. C. Davies, Cystic fibrosis. *Lancet* **397**, 2195–2211 (2021).
3. P. J. Barnes, New drugs for asthma. *Nat. Rev. Drug Discov.* **3**, 831–844 (2004).
4. L. A. Vijftigschild, G. Berkers, J. F. Dekkers, D. D. Zomer-van Ommen, E. Matthes, E. Kruisselbrink, A. Vonk, C. E. Hensen, S. Heida-Michel, M. Geerdink, H. M. Janssens, E. A. van de Graaf, I. Bronsveld, K. M. de Winter-de Groot, C. J. Majoor, H. G. Heijerman, H. R. de Jonge, J. W. Hanrahan, C. K. van der Ent, J. M. Beekman, β 2-Adrenergic receptor agonists activate CFTR in intestinal organoids and subjects with cystic fibrosis. *Eur. Respir. J.* **48**, 768–779 (2016).
5. E. M. Dunican, B. M. Elicker, T. Henry, D. S. Gierada, M. L. Schiebler, W. Anderson, I. Barjaktarevic, R. G. Barr, E. R. Blecker, R. C. Boucher, R. Bowler, S. A. Christenson, A. Comellas, C. B. Cooper, D. Couper, G. J. Criner, M. Dransfield, C. M. Doerschuk, M. B. Drummond, N. N. Hansel, M. K. Han, A. T. Hastie, E. A. Hoffman, J. A. Krishnan, S. C. Lazarus, F. J. Martinez, C. E. McCulloch, W. K. O'Neal, V. E. Ortega, R. Paine III, S. Peters, J. D. Schroeder, P. G. Woodruff, J. V. Fahy, Mucus plugs and emphysema in the pathophysiology of airflow obstruction and hypoxemia in smokers. *Am. J. Respir. Crit. Care Med.* **203**, 957–968 (2021).
6. E. M. Dunican, B. M. Elicker, D. S. Gierada, S. K. Nagle, M. L. Schiebler, J. D. Newell, W. W. Raymond, M. E. Lachowicz-Scroggins, S. Di Maio, E. A. Hoffman, M. Castro, S. B. Fain, N. N. Jarjour, E. Israel, B. D. Levy, S. C. Erzurum, S. E. Wenzel, D. A. Meyers, E. R. Blecker, B. R. Phillips, D. T. Mauger, E. D. Gordon, P. G. Woodruff, M. C. Peters, J. V. Fahy; National Heart Lung and Blood Institute (NHLBI) Severe Asthma Research Program, Mucus plugs in patients with asthma linked to eosinophilia and airflow obstruction. *J. Clin. Invest.* **128**, 997–1009 (2018).
7. D. H. Maurice, H. Ke, F. Ahmad, Y. Wang, J. Chung, V. C. Manganiello, Advances in targeting cyclic nucleotide phosphodiesterases. *Nat. Rev. Drug Discov.* **13**, 290–314 (2014).

8. Y. Oba, Phosphodiesterase inhibitors in chronic obstructive pulmonary disease. *Am. J. Respir. Crit. Care Med.* **188**, 1366 (2013).
9. A. Ghigo, A. Perino, H. Mehel, A. Zahradnikova Jr., F. Morello, J. Leroy, V. O. Nikolaev, F. Damilano, J. Cimino, E. De Luca, W. Richter, R. Westenbroek, W. A. Catterall, J. Zhang, C. Yan, M. Conti, A. M. Gomez, G. Vandecasteele, E. Hirsch, R. Fischmeister, Phosphoinositide 3-kinase γ protects against catecholamine-induced ventricular arrhythmia through protein kinase A-mediated regulation of distinct phosphodiesterases. *Circulation* **126**, 2073–2083 (2012).
10. A. Perino, A. Ghigo, E. Ferrero, F. Morello, G. Santulli, G. S. Baillie, F. Damilano, A. J. Dunlop, C. Pawson, R. Walsler, R. Levi, F. Altruda, L. Silengo, L. K. Langeberg, G. Neubauer, S. Heymans, G. Lembo, M. P. Wymann, R. Wetzker, M. D. Houslay, G. Iaccarino, J. D. Scott, E. Hirsch, Integrating cardiac PIP3 and cAMP signaling through a PKA anchoring function of p110 γ . *Mol. Cell* **42**, 84–95 (2011).
11. V. Fanelli, V. Puntorieri, B. Assenzio, E. L. Martin, V. Elia, M. Bosco, L. Delsedime, L. Del Sorbo, A. Ferrari, S. Italiano, A. Ghigo, A. S. Slutsky, E. Hirsch, V. M. Ranieri, Pulmonary-derived phosphoinositide 3-kinase gamma (PI3K γ) contributes to ventilator-induced lung injury and edema. *Intensive Care Med.* **36**, 1935–1945 (2010).
12. G. Guidotti, L. Brambilla, D. Rossi, Cell-penetrating peptides: From basic research to clinics. *Trends Pharmacol. Sci.* **38**, 406–424 (2017).
13. C. Laudanna, J. J. Campbell, E. C. Butcher, Elevation of intracellular cAMP inhibits RhoA activation and integrin-dependent leukocyte adhesion induced by chemoattractants. *J. Biol. Chem.* **272**, 24141–24144 (1997).
14. E. Blanchard, L. Zlock, A. Lao, D. Mika, W. Namkung, M. Xie, C. Scheitrum, D. C. Gruenert, A. S. Verkman, W. E. Finkbeiner, M. Conti, W. Richter, Anchored PDE4 regulates chloride conductance in wild-type and Δ F508-CFTR human airway epithelia. *FASEB J.* **28**, 791–801 (2014).
15. A. Schnur, A. Premchand, M. Bagdany, G. L. Lukacs, Phosphorylation-dependent modulation of CFTR macromolecular signalling complex activity by cigarette smoke condensate in airway epithelia. *Sci. Rep.* **9**, 12706 (2019).
16. T. Hegedus, A. Aleksandrov, A. Mengos, L. Cui, T. J. Jensen, J. R. Riordan, Role of individual R domain phosphorylation sites in CFTR regulation by protein kinase A. *Biochim. Biophys. Acta* **1788**, 1341–1349 (2009).
17. S. L. Martin, V. Saint-Criq, T. C. Hwang, L. Csanady, Ion channels as targets to treat cystic fibrosis lung disease. *J. Cyst. Fibros.* **17**, S22–S27 (2018).
18. J. F. Dekkers, C. L. Wiegierinck, H. R. de Jonge, I. Bronsveld, H. M. Janssens, K. M. de Winter-de Groot, A. M. Brandsma, N. W. de Jong, M. J. Bijvelds, B. J. Scholte, E. E. Nieuwenhuis, S. van den Brink, H. Clevers, C. K. van der Ent, S. Middendorp, J. M. Beekman, A functional CFTR assay using primary cystic fibrosis intestinal organoids. *Nat. Med.* **19**, 939–945 (2013).
19. D. M. Cholon, N. L. Quinney, M. L. Fulcher, C. R. Esther Jr., J. Das, N. V. Dokholyan, S. H. Randell, R. C. Boucher, M. Gentszsch, Potentiator ivacaftor abrogates pharmacological correction of Δ F508 CFTR in cystic fibrosis. *Sci. Transl. Med.* **6**, 246ra96 (2014).
20. A. Lupieri, R. Blaise, A. Ghigo, N. Smirnova, M. K. Sarthou, N. Malet, I. Limon, P. Vincent, E. Hirsch, S. Gayral, D. Ramel, M. Laffargue, A non-catalytic function of PI3K γ drives smooth muscle cell proliferation after arterial damage. *J. Cell Sci.* **133**, jcs245969 (2020).
21. H. Zuo, I. Cattani-Cavaliere, N. Musheshe, V. O. Nikolaev, M. Schmidt, Phosphodiesterases as therapeutic targets for respiratory diseases. *Pharmacol. Ther.* **197**, 225–242 (2019).
22. C. Mehats, S. L. Jin, J. Wahlstrom, E. Law, D. T. Umetsu, M. Conti, PDE4D plays a critical role in the control of airway smooth muscle contraction. *FASEB J.* **17**, 1831–1841 (2003).
23. C. K. Billington, I. R. Le Jeune, K. W. Young, I. P. Hall, A major functional role for phosphodiesterase 4D5 in human airway smooth muscle cells. *Am. J. Respir. Cell Mol. Biol.* **38**, 1–7 (2008).
24. A. Ray, J. K. Kolls, Neutrophilic inflammation in asthma and association with disease severity. *Trends Immunol.* **38**, 942–954 (2017).
25. A. Butler, G. M. Walton, E. Sapey, Neutrophilic inflammation in the pathogenesis of chronic obstructive pulmonary disease. *COPD* **15**, 392–404 (2018).
26. L. Abou Saleh, A. Boyd, I. V. Aragon, A. Koloteva, D. Spadafora, W. Mneimneh, R. A. Barrington, W. Richter, Ablation of PDE4B protects from *Pseudomonas aeruginosa*-induced acute lung injury in mice by ameliorating the cytoskeleton and associated hyperthermia. *FASEB J.* **35**, e21797 (2021).
27. M. J. Turner, K. Abbott-Banner, D. Y. Thomas, J. W. Hanrahan, Cyclic nucleotide phosphodiesterase inhibitors as therapeutic interventions for cystic fibrosis. *Pharmacol. Ther.* **224**, 107826 (2021).
28. S. D. Patel, T. R. Bono, S. M. Rowe, G. M. Solomon, CFTR targeted therapies: Recent advances in cystic fibrosis and possibilities in other diseases of the airways. *Eur. Respir. Rev.* **29**, 190068 (2020).
29. M. J. Turner, Y. Luo, D. Y. Thomas, J. W. Hanrahan, The dual phosphodiesterase 3/4 inhibitor RPL554 stimulates rare class III and IV CFTR mutants. *Am. J. Physiol. Lung Cell. Mol. Physiol.* **318**, L908–L920 (2020).
30. H. Vais, R. Zhang, W. W. Reenstra, Dibasic phosphorylation sites in the R domain of CFTR have stimulatory and inhibitory effects on channel activation. *Am. J. Physiol. Cell Physiol.* **287**, C737–C745 (2004).
31. O. Baldursson, H. A. Berger, M. J. Welsh, Contribution of R domain phosphoserines to the function of CFTR studied in Fischer rat thyroid epithelia. *Am. J. Physiol. Lung Cell. Mol. Physiol.* **279**, L835–L841 (2000).
32. S. Chin, M. Hung, C. E. Bear, Current insights into the role of PKA phosphorylation in CFTR channel activity and the pharmacological rescue of cystic fibrosis disease-causing mutants. *Cell. Mol. Life Sci.* **74**, 57–66 (2017).
33. P. D. Eckford, C. Li, M. Ramjeeasingh, C. E. Bear, Cystic fibrosis transmembrane conductance regulator (CFTR) potentiator VX-770 (ivacaftor) opens the defective channel gate of mutant CFTR in a phosphorylation-dependent but ATP-independent manner. *J. Biol. Chem.* **287**, 36639–36649 (2012).
34. M. A. Mall, N. Mayer-Hamblett, S. M. Rowe, Cystic fibrosis: Emergence of highly effective targeted therapeutics and potential clinical implications. *Am. J. Respir. Crit. Care Med.* **201**, 1193–1208 (2020).
35. G. Veit, A. Roldan, M. A. Hancock, D. F. Da Fonte, H. Xu, M. Hussein, S. Frenkiel, E. Matouk, T. Velkov, G. L. Lukacs, Allosteric folding correction of F508del and rare CFTR mutants by elxacaftor-tezacaftor-ivacaftor (Trikafta) combination. *JCI Insight* **5**, e139983 (2020).
36. I. d'Angelo, C. Conte, M. I. La Rotonda, A. Miro, F. Quaglia, F. Ungaro, Improving the efficacy of inhaled drugs in cystic fibrosis: Challenges and emerging drug delivery strategies. *Adv. Drug Deliv. Rev.* **75**, 92–111 (2014).
37. C. B. Morrison, K. M. Shaffer, K. C. Araba, M. R. Markovetz, J. A. Wykoff, N. L. Quinney, S. Hao, M. F. Delion, A. L. Flen, L. C. Morton, J. Liao, D. B. Hill, M. L. Drumm, W. K. O'Neal, M. Kesimer, M. Gentszsch, C. Ehre, Treatment of cystic fibrosis airway cells with CFTR modulators reverses aberrant mucus properties via hydration. *Eur. Respir. J.* 2100185 (2022).
38. E. Hirsch, V. L. Katanaev, C. Garlanda, O. Azzolino, L. Pirola, L. Silengo, S. Sozzani, A. Mantovani, F. Altruda, M. P. Wymann, Central role for G protein-coupled phosphoinositide 3-kinase gamma in inflammation. *Science* **287**, 1049–1053 (2000).
39. E. Patrucco, A. Notte, L. Barberis, G. Selvetella, A. Maffei, M. Brancaccio, S. Marengo, G. Russo, O. Azzolino, S. D. Rybalkin, L. Silengo, F. Altruda, R. Wetzker, M. P. Wymann, G. Lembo, E. Hirsch, PI3Kgamma modulates the cardiac response to chronic pressure overload by distinct kinase-dependent and -independent effects. *Cell* **118**, 375–387 (2004).
40. L. M. DiPilato, J. Zhang, The role of membrane microdomains in shaping beta2-adrenergic receptor-mediated cAMP dynamics. *Mol. Biosyst.* **5**, 832–837 (2009).
41. A. Terrin, G. Di Benedetto, V. Pertegato, Y. F. Cheung, G. Baillie, M. J. Lynch, N. Elvassore, A. Prinz, F. W. Herberg, M. D. Houslay, M. Zaccolo, PGE(1) stimulation of HEK293 cells generates multiple contiguous domains with different [cAMP]: Role of compartmentalized phosphodiesterases. *J. Cell Biol.* **175**, 441–451 (2006).
42. B. Ponsioen, J. Zhao, J. Riedl, F. Zwartkruis, G. van der Krogt, M. Zaccolo, W. H. Moolenaar, J. L. Bos, K. Jalink, Detecting cAMP-induced Epac activation by fluorescence resonance energy transfer: Epac as a novel cAMP indicator. *EMBO Rep.* **5**, 1176–1180 (2004).
43. W. J. Thompson, M. M. Appleman, Characterization of cyclic nucleotide phosphodiesterases of rat tissues. *J. Biol. Chem.* **246**, 3145–3150 (1971).
44. G. Di Benedetto, A. Zoccarato, V. Lissandron, A. Terrin, X. Li, M. D. Houslay, G. S. Baillie, M. Zaccolo, Protein kinase A type I and type II define distinct intracellular signaling compartments. *Circ. Res.* **103**, 836–844 (2008).
45. R. A. Cardone, A. Bagorda, A. Bellizzi, G. Busco, L. Guerra, A. Paradiso, V. Casavola, M. Zaccolo, S. J. Reshkin, Protein kinase A gating of a pseudopodial-located RhoA/ROCK/p38/NHE1 signal module regulates invasion in breast cancer cell lines. *Mol. Biol. Cell* **16**, 3117–3127 (2005).
46. K. L. Holmes, L. M. Lantz, W. Russ, Conjugation of fluorochromes to monoclonal antibodies. *Curr. Protoc. Cytom.* **Chapter 4**, Unit 4.2 (2001).
47. G. T. Hermanson, *Bioconjugate Techniques* (2008).
48. D. W. McGraw, S. L. Forbes, L. A. Kramer, D. P. Witte, C. N. Fortner, R. J. Paul, S. B. Liggett, Transgenic overexpression of β 2-adrenergic receptors in airway smooth muscle alters myocyte function and ablates bronchial hyperreactivity. *J. Biol. Chem.* **274**, 32241–32247 (1999).
49. M. Matthey, R. Roberts, A. Seidinger, A. Simon, R. Schroder, M. Kuschak, S. Annala, G. M. Konig, C. E. Muller, I. P. Hall, E. Kostenis, B. K. Fleischmann, D. Wenzel, Targeted inhibition of G $_q$ signaling induces airway relaxation in mouse models of asthma. *Sci. Transl. Med.* **9**, eaag2288 (2017).
50. C. Laudanna, J. J. Campbell, E. C. Butcher, Role of Rho in chemoattractant-activated leukocyte adhesion through integrins. *Science* **271**, 981–983 (1996).
51. M. Bolomini-Vittori, A. Montresor, C. Giagulli, D. Staunton, B. Rossi, M. Martinello, G. Constantin, C. Laudanna, Regulation of conformer-specific activation of the integrin LFA-1 by a chemokine-triggered Rho signaling module. *Nat. Immunol.* **10**, 185–194 (2009).
52. M. Li, V. Sala, M. C. De Santis, J. Cimino, P. Cappello, N. Pianca, A. Di Bona, J. P. Margaria, M. Martini, E. Lazzarini, F. Pirozzi, L. Rossi, I. Franco, J. Bornbaum, J. Heger, S. Rohrbach,

- A. Perino, C. G. Tocchetti, B. H. F. Lima, M. M. Teixeira, P. E. Porporato, R. Schulz, A. Angelini, M. Sandri, P. Ameri, S. Sciarretta, R. C. P. Lima-Junior, M. Mongillo, T. Zaglia, F. Morello, F. Novelli, E. Hirsch, A. Ghigo, Phosphoinositide 3-kinase gamma inhibition protects from anthracycline cardiotoxicity and reduces tumor growth. *Circulation* **138**, 696–711 (2018).
53. A. Premchandrar, A. Kupniewska, A. Bonna, G. Faure, T. Fraczyk, A. Roldan, B. Hoffmann, M. Faria da Cunha, H. Herrmann, G. L. Lukacs, A. Edelman, M. Dadlez, New insights into interactions between the nucleotide-binding domain of CFTR and keratin 8. *Protein Sci.* **26**, 343–354 (2017).
54. V. Montiel, R. Bella, L. Y. M. Michel, H. Esfahani, D. De Mulder, E. L. Robinson, J. P. Deglasse, M. Tiburcy, P. H. Chow, J. C. Jonas, P. Gilon, B. Steinhorn, T. Michel, C. Beauloye, L. Bertrand, C. Farah, F. D. Zotti, H. Debaix, C. Bouzin, D. Brusa, S. Horman, J. L. Vanoverschelde, O. Bergmann, D. Gilis, M. Rooman, A. Ghigo, S. Geninatti-Crich, A. Yool, W. H. Zimmermann, H. L. Roderick, O. Devuyt, J. L. Balligand, Inhibition of aquaporin-1 prevents myocardial remodeling by blocking the transmembrane transport of hydrogen peroxide. *Sci. Transl. Med.* **12**, eaay2176 (2020).
55. M. R. Ruggiero, S. Baroni, S. Pezzana, G. Ferrante, S. Geninatti Crich, S. Aime, Evidence for the role of intracellular water lifetime as a tumour biomarker obtained by in vivo field-cycling relaxometry. *Angew. Chem. Int. Ed. Engl.* **57**, 7468–7472 (2018).
56. E. Terreno, S. Geninatti Crich, S. Belfiore, L. Biancone, C. Cabella, G. Esposito, A. D. Manazza, S. Aime, Effect of the intracellular localization of a Gd-based imaging probe on the relaxation enhancement of water protons. *Magn. Reson. Med.* **55**, 491–497 (2006).
57. P. Scudieri, I. Musante, E. Caci, A. Venturini, P. Morelli, C. Walter, D. Tosi, A. Palleschi, P. Martin-Vasallo, I. Sermet-Gaudelus, G. Planelles, G. Crambert, L. J. Galletta, Increased expression of ATP12A proton pump in cystic fibrosis airways. *JCI Insight* **3**, e123616 (2018).
58. L. Zhang, M. Gallup, L. Zlock, W. E. Finkbeiner, N. A. McNamara, Rac1 and Cdc42 differentially modulate cigarette smoke-induced airway cell migration through p120-catenin-dependent and -independent pathways. *Am. J. Pathol.* **182**, 1986–1995 (2013).
59. M. Xie, T. C. Rich, C. Scheitrum, M. Conti, W. Richter, Inactivation of multidrug resistance proteins disrupts both cellular extrusion and intracellular degradation of cAMP. *Mol. Pharmacol.* **80**, 281–293 (2011).
60. G. Veit, F. Bossard, J. Goepp, A. S. Verkman, L. J. Galletta, J. W. Hanrahan, G. L. Lukacs, Proinflammatory cytokine secretion is suppressed by TMEM16A or CFTR channel activity in human cystic fibrosis bronchial epithelia. *Mol. Biol. Cell* **23**, 4188–4202 (2012).
- the NIH (P30DK065988 to M.G.), Cystic Fibrosis Canada and FRQS Postdoctoral Fellowship (to A.P.), Canadian Institute for Health Research (CIHR) (PJT 153095 to G.L.L.), Cystic Fibrosis Foundation (CFF) (00988G220 to G.L. and BOUCHE15R0 to M.G.), Cystic Fibrosis Canada (to G.L.L.), and the German Federal Ministry of Education and Research (82DZL009B1 to M.A.M.).
- Author contributions:** A. Ghigo and E.H. conceived and designed the overall study. A. Ghigo and A. Murabito carried out the core of the experiments and analyzed the data. V.S., A.R.P., and S. Bertolini performed immunoprecipitation and immunoblotting assays. A. Gianotti, E.C., W.R., and N.L.Q. performed short-circuit current measurements in Ussing chambers. A. Montresor performed all experiments with human neutrophils. A.P. performed CFTR phosphoproteomic experiments. F.P. and R.K. carried out all experiments with OVA-sensitized mice. A.D.S. carried out all experiments with macrophages. M. Mergioti, M.R.R., and S. Baroni measured water residence time. E.d.P. and S.C. carried out FIS assays in organoids. M. Matthey and A.C. carried out lung function measurements. R.A.C. performed FRET-based cAMP measurements in epithelial cells. F.C. measured tracheal ring contractility. C.B. measured PI3Kγ MP/PKA-RII dissociation constant. S.V., S.G.C., D.R., M.L., C.G.T., R.L., M.C., X.L., P.M., C.S., V.D.R., F.F., V.F., D.W., B.K.F., M.A.M., J.B., C.L., M.G., G.L.L., and N.P. provided advice on the interpretation of data. A. Ghigo, A. Murabito, and E.H. wrote the manuscript with input from coauthors. All authors reviewed and approved the final manuscript. **Competing interests:** A. Ghigo and E.H. are cofounders and board members of Kither Biotech Srl. A. Ghigo and E.H. are coinventors of patent titled “Novel pi3k gamma inhibitor peptide for treatment of respiratory system diseases” (WO2016103176A1) that is directly associated with the study. M.A.M. reports personal fees for participation in advisory boards or paid consulting from Abbvie, Antabio, Arrowhead Pharmaceuticals, Boehringer Ingelheim, Enterprise Therapeutics, Kither Biotech, Pieris Pharmaceuticals, Santhera, Sterna Biologicals, and Vertex Pharmaceuticals outside the submitted work. P.M. declares consulting activities paid by Kither Biotech and expert testimony fees paid by Vertex Pharmaceuticals. J.B. is inventor on a patent related to organoid swelling and received financial royalties for this contribution from the Royal Dutch Academy of Sciences and Arts. All other authors declare that they have no competing interests. **Data and materials availability:** All data associated with this study are available in the paper or the Supplementary Materials. Individual values and data from main and supplementary figures are presented in data files S1 and S2, respectively. PI3Kγ MP is available to the scientific community upon completion of a material transfer agreement with Kither Biotech Srl. The following cell lines and reagents were obtained through a material transfer agreement between University of Torino and the indicated institution: 16HBE14o- and CFBE41o- cells (University of California San Francisco), wt-CFTR-CFBE41o- and F508del-CFTR-CFBE41o- (University of Alabama at Birmingham), and CFTR antibodies (University of North Carolina–Chapel Hill).

Acknowledgments: We would like to thank E. Balmas and L. Conti for discussions. **Funding:** This work was supported by research grants from the Italian Cystic Fibrosis Research Foundation (FFC#25/2014 to E.H., FFC#23/2015 to E.H., FFC#8/2018 to E.H., FFC#4/2016 to A. Ghigo, and FFC#11/2017 to A. Ghigo), Cariplo Foundation (#2015-0880 to A. Ghigo and #2018-0498 to E.H.), Roche Foundation (Bando Roche per la Ricerca 2019 to A. Ghigo), Compagnia di San Paolo (CSTO161109 to E.H.), Telethon Foundation (GGP20079 to A. Ghigo.),

Submitted 2 August 2021
Resubmitted 26 November 2021
Accepted 25 February 2022
Published 30 March 2022
10.1126/scitranslmed.abl6328

A PI3K# mimetic peptide triggers CFTR gating, bronchodilation, and reduced inflammation in obstructive airway diseases

Alessandra GhigoAlessandra MurabitoValentina SalaAnna Rita PisanoSerena BertoliniAmbra GianottiEmanuela CaciAlessio MontresorAiswarya PremchandarFlora PirozziKai RenAngela Della SalaMarco MergiottiWito RichterEyleen de PoelMichaela MattheySara CaldreaRosa A. CardoneFederica CivilettiAndrea CostamagnaNancy L. QuinneyCosmin ButnaruSonja VisentinMaria Rosaria RuggieroSimona BaroniSimonetta GeninattiCrichDamien RamelMuriel LaffargueCarlo G. TocchettiRenzo LeviMarco ContiXiao-Yun LuPaola MelottiClaudio SorioVirginia De RoseFabrizio FacchinettiVito FanelliDaniela WenzelBernd K. FleischmannMarcus A. MallJeffrey BeekmanCarlo LaudannaMartina GentzschGergely L. LukacsNicoletta PedemonteEmilio Hirsch

Sci. Transl. Med., 14 (638), eabl6328. • DOI: 10.1126/scitranslmed.abl6328

PI3K-ing a mimetic

Increasing cyclic adenosine monophosphate (cAMP) in the airways of patients with obstructive lung diseases can reduce airway inflammation and constriction. However, current therapies can induce treatment-limiting systemic side effects. Here, Ghigo and colleagues found that phosphoinositide 3-kinase # (PI3K#) negatively regulated the #-adrenergic receptor signaling pathway to decrease cAMP. They created a PI3K# mimetic peptide that increased local cAMP concentrations and, when administered intratracheally in a mouse model of asthma, induced airway relaxation and reduced neutrophil infiltration. Further, in airway epithelial cells from patients with cystic fibrosis, it triggered gating of the cystic fibrosis transmembrane conductance regulator (CFTR) channel and enhanced the effects of CFTR modulators, suggesting that the PI3K# mimetic peptide may be used to treat obstructive lung diseases in humans.

View the article online

<https://www.science.org/doi/10.1126/scitranslmed.abl6328>

Permissions

<https://www.science.org/help/reprints-and-permissions>

Use of this article is subject to the [Terms of service](#)